Modeling of Metamaterials in Wave Propagation

G. Leugering, E. Rohan and F. Seifrt

Lehrstuhl für Angewandte Mathematik II, Universität Erlangen-Nürnberg, Germany.
New Technologies Research Center, Research Institute at University of West Bohemia, Plzen, Czech Republic.

Abstract: This chapter focuses on acoustic, electromagnetic, elastic and piezo-electric wave propagation through heterogenous layers. The motivation is provided by the demand for a better understanding of meta-materials and their possible construction. We stress the analogies between the mathematical treatment of phononic, photonic and elastic meta-materials. Moreover, we treat the cloaking problem in more detail from an analytical and simulation oriented point of view. The novelty in the approach presented here is with the interlinked homogenization- and optimization procedure.

INTRODUCTION

The terminology 'metamaterials' refers to 'beyond conventional material properties' and consequently those 'materials' typically are not found in nature. It comes as no surprise that research in this area, once the first examples became publicly known, has undergone an exponential growth. Metamaterials are most often man-made, are engineered materials with a wide range of applications. Starting in the area of micro-waves where one aims at cloaking objects from electromagnetic waves in the invisible frequency range, the ideas rather quickly inflicted researcher from optics for a variety of reasons. Superlenses allowing nanoscale imaging and nanophotolithography, couple light to the nanoscale yielding a family of negative-index-material(NIM)-based devices for nanophotonics, such as nanoscale antennae, resonators, lasers, switchers, waveguides and finally cloaking are just the most prominent fascinating fields. Nano-structured materials are characterized by 'ultra-fine microstructure'. There are at least two reasons why downscaling the size of a microstructure can drastically influence its properties. 'First, as grain size gets smaller, the proportion of atoms at grain boundaries or on surfaces increases rapidly. The other reason is related to the fact that many physical phenomena (such as dislocation generation, ferromagnetism, or quantum confinement effects) are governed by a characteristic length. As the physical scale of the material falls below this length, properties change radically'(see [44]).

Metamaterial properties, therefore, emerge under the controlled influence of microstructures. Inclusions on the nano-scale together with their material properties and their shape are to be designed in order to fulfill certain desired material properties, such as 'negative Poisson' ratio in elastic material foams, negative 'mass' and 'negative refraction indices' for the forming of band-gaps in acoustic and optical devices, respectively.

Thus given acoustic, elasto-dynamic, piezo-electric or electromagnetic wave propagation in a non-homogeneous medium and given a certain merit function describing the desired material-property or dynamic performance of the body involved, one wants to find e.g. the location, size, shape and material properties of small inclusions such that the merit function is increased towards an optimal material or performance. This, at the the first glance, sounds like the formulation of an ancient dream of man-kind. However, proper mathematical modelling, thorough mathematical analysis together with a model-based optimization and simulation can, when accompanied by experts in optics and engineering, lead to such metamaterial-concepts and finally to products.

Designing optimal microstructures can be seen from two aspects. Firstly, inclusions, their size, positions and properties are considered on a finite, say, nano-scale and are subject to shape, topology and material optimization. Secondly, such potential microstructures are seen from the macroscopic scale in form of some effective or averaged material. This brings in the notion and the theory of homogenization of microstructures. The interplay between homogenization and optimization becomes, thus, most prominent.

Besides the optimal design approach to metamaterial, in particular in the context of negative refraction indices, permittivities, permeabilities, there is another fascinating branch of research that concentrates on 'Transformation Optics', a notion promoted by Pendry et.al. [27, 45] in optics and Greenleaf et.al. [16] in the more mathematically inclined literature. We refrain from attempting any recollection of major contribution to this field and refer to these survey articles ([27, 45, 16]) and the references therein. In order to be more specific and because in this contribution we will not dwell on this approach on any research level, we give a brief account of the underlying idea.

Cloaking problem and metamaterials: transformation method

In order to keep matters as simple as possible, we consider the following classical problem

$$\begin{cases} \nabla\cdot\sigma\nabla u = 0, & \text{in } \Omega, \\ u = f, & \text{on } \partial\Omega. \end{cases} \tag{1}$$

We have the *Dirichlet-to-Neumann map* (DtN)

$$\Lambda_\sigma(f) := \nu\cdot\sigma\nabla u|_{\partial\Omega}. \tag{2}$$

Calderón's problem is then to reconstruct σ from Λ_σ! For smooth and isotropic σ this is possible. Thus, in that case the Cauchy data $(f,\Lambda_\sigma(f))$ uniquely determine σ. Therefore, no cloaking is possible with smooth variations of the material! In the heterogeneous an-isotropic case, we may consider a diffeomorphism $F:\Omega\to\Omega$ with $F|_{\partial\Omega}=I$ and then make a change of variables $y=F(x)$ s.t. $u=v\circ F^{-1}$. The so-called push forward is defined as

$$\begin{aligned} (F_*\sigma)^{jk}(y) &:= \frac{1}{\det DF_{jk}} S^{jk}(x)|_{x=F^{-1}(y)} \\ S^{jk}(x) &:= \sum_{p,q=1}^{n} \frac{\partial F^j}{\partial x^p}(x)\frac{\partial F^k}{\partial x^q}(x)\sigma^{pq}(x). \end{aligned} \tag{3}$$

We notice that

$$\Lambda_\sigma = \Lambda_{F_*\sigma}, \tag{4}$$

where DF_{jk} denotes the Jacobi-matrix of F ($DF=\nabla F^T$). The idea behind is that the coefficients σ can be interpreted as a Riemann metric. Transformations into curvilinear coordinates are classic in mechanics, see e.g. Gurtin[17]. Thus, transformations into curvilinear coordinates correspond one-to-one with transformation between different materials. The construction of a transformation that allows for cloaking is as follows.

Denote $\hat{x}:=\frac{x}{|x|}$, $\hat{y}:=\frac{y}{|y|}$ and define the mapping $F:\mathbb{R}^3\setminus\{0\}\to\mathbb{R}^3\setminus\{B_a(0)\}$

$$x=F(y):=\begin{cases} x=x(y)=f(y):=g(|y|)\hat{y}, \\ \quad \text{for } 0<|y|\le b, \\ x=x(y):=y, \text{ for } |y|>b, \end{cases} \tag{5}$$

where $B_r(x_0):=\{x\in\mathbb{R}^3 : |x-x_0|\le r\}$ and such that g satisfies: for a,b with $0<a<b$, $g\in C^2([0,b])$, $g(0)=a$, $g(b)=b$ and $g'(\rho)>0$, $\forall\rho\in[0,b]$ This transformation maps the punctuated three-space into a spherical ring with inner radius a and outer radius b, such that the exterior of the ball $B_b(0)$ is left unchanged. We consider the ball $K:=B_a(0)$ as the cloaked object, the layer $\{x : a<|x|\le b\}$ as the cloaking layer and the union as the spherical cloak. The shape of the cloak can be arbitrary, however. Examples for spherical cloaks are $g(\rho):=\frac{b-a}{b}\rho+a$ (linear) or $g(\rho):=\left[1-\frac{a}{b}+p(\rho-b)\right]\rho+a$ (quadratic)

We consider a similar construction as above, but now for many cloaked objects located at point $c_i, i=1,\dots,N$:

$$x=F(y):=\begin{cases} f(y):=c_i+g_i(|y-c_i|)(\hat{y}-c_i), \\ \quad \text{for } y\in B_{b_i}(c_i),\ i=1,\dots,N \\ y, \text{ for } y\in\mathbb{R}^3_0\setminus\{\cup_{i=1}^N B_{b_i}(c_i)=:\tilde{\Omega}\}, \end{cases} \tag{6}$$

where the cloaked objects are now

$$K_i:=\{x\in\mathbb{R}^3 : |x-c_i|\le a_i\}, i=1,\dots N \tag{7}$$

$K=\cup_{i=1}^N K_i$ is the entire cloaked object. The cloaked subregions are supposed to be separated:

$$\min\operatorname{dist}(B_{b_i}(c_i),B_{b_j}(c_j))>0,\ \forall i\ne j,\ i,j=1,\dots,N \tag{8}$$

The domains of interest are now: $\Omega_0:=\mathbb{R}^3\setminus\{c_1,\dots,c_N\}$, $\Omega:=\mathbb{R}^3\setminus K$. $F(\cdot)$ is only piecewise smooth with singularities across ∂K.

$$DF(y)_{kl}=\begin{cases} \frac{g_j(|y-c_j|)}{|y-c_j|}\delta_{kl}+\left(\frac{g_j'(|y-c_j|)}{|y-c_j|^2}-\frac{g_j(|y-c_j|)}{|y-c_j|^3}\right)\cdot \\ \quad\cdot(y-c_j)_k(y-c_j)_l, y\in B_{b_J}(c_j) \\ \delta_{kl}, y\in\tilde{\Omega} \end{cases} \tag{9}$$

We have the determinant $\Delta(y)=\det DF(y)$

$$\Delta(y)=\begin{cases} g_j'(|y-c_j|)\left(\frac{g_j(|y-c_j|)}{|y-c_j|}\right)^2, \\ \quad y\in B_{b_j}(c_j), j=1,\dots,N \\ 1, y\in\tilde{\Omega} \end{cases} \tag{10}$$

It is obvious that $\sigma_*=F_*\sigma$ is degenerate along the boundary ∂K. Thus, in order to properly pose a self-adjoint extension of the corresponding Laplace(-Beltrami-)operator, we need to work in weighted spaces.

The idea above is extended to the phononic and the photonic situation. In particular treating the Maxwell system in its time-harmonic form the transformed system reads as

$$\nabla \times \boldsymbol{E} = \mathrm{j}k\mu(x)\boldsymbol{H}, \quad \nabla \times \boldsymbol{H} = -\mathrm{j}k\varepsilon(x)\boldsymbol{H} + \boldsymbol{J}_e \tag{11}$$

where ε, μ are given by:

$$\varepsilon = \frac{1}{\Delta(y)} D^T F \varepsilon_0 DF, \; \mu = \frac{1}{\Delta(y)} DF^T \mu_0 DF \tag{12}$$

The material matrices ε, μ are again degenerate at ∂K!

In order to obtain finite energy solutions to the Maxwell system, one needs to work in weighted spaces. For cloaking, one requires energy conservation. Introduce weighted scalar products

$$\begin{aligned}(\boldsymbol{E}^1, \boldsymbol{E}^2)_{\Omega,E} &:= \int_\Omega \boldsymbol{E}^1 \cdot \varepsilon \bar{\boldsymbol{E}}^2 dx, \; (\boldsymbol{H}^1, \boldsymbol{H}^2)_{\Omega,H} \\ &= \int_\Omega \boldsymbol{H}^1 \cdot \mu \bar{\boldsymbol{H}}^2 dx\end{aligned} \tag{13}$$

and require local energy conservation. To this end define the local energy for an open bounded subdomain $O \subset \Omega$

$$\int_\Omega \boldsymbol{E} \cdot \varepsilon \bar{\boldsymbol{E}} dx + \int_\Omega \boldsymbol{H} \cdot \mu \bar{\boldsymbol{H}} dx < \infty. \tag{14}$$

A solution satisfies the Maxwell system in the distributional sense and has finite local energy. One obtains **two** boundary (over-determined i.g.) conditions on ∂K

$$\begin{aligned}\boldsymbol{E} \times \boldsymbol{n} = 0, \; \boldsymbol{H} \times \boldsymbol{n} = 0, \; &\text{on } \partial K_+, \\ (\nabla \times \boldsymbol{E}) \cdot \boldsymbol{n} = 0, \; (\nabla \times \boldsymbol{H}) \cdot \boldsymbol{n} = 0, \; &\text{on } \partial K_-,\end{aligned} \tag{15}$$

This procedure of defining cloaking transformations is rather general and applies also to elliptic systems, 2-d and 3-d elasticity, elasto-dynamics and the time-dependent Maxwell equations. Thus, formally, from a purely mathematical point of view, the problem of cloaking can be regarded as analytically solved. The fundamental question however remains: How can the transformed material tensors be realized ?

Indeed, this problem is widely open. There is an approach to approximate the cloaking transforms by less singular mappings in particular by inflating a ball rather than a point to a ring-shaped domain. But still, the material could not be realized so far and further analysis is in order. On the positive side it is evident that even from the point of view of transformation optics the appearance of singular behaviour at the boundary of the region to be cloaked indicates that microstructures may genuinely occur. Indeed, a second approach [16] is based on a truncation of ε, μ to such tensors, say ε_R, μ_R that are uniformly (in x) bounded above and below. When $R \to 1$ they tend to ε, μ, respectively. It is shown in [16] that it is possible to match these tensors ε_R, μ_R by periodic microstructured material in the cloak in the homogenization limit. The result shows that utopian 'metamaterial' constructed by an approximation to exact cloaking can be 'realized' via homogenization of periodic microstructures within the cloaking region. This is a very encouraging result that needs to be further exploited.

Metamaterials via homogenization

In this contribution we want to discuss the theme of object cloaking by 'homogenized metamaterials'. We are aiming at designing coating layers containing microstructure which are 'wrapped' around an object. The coated object may be subject to acoustic or electromagnetic incoming waves. We want to survey and present new results applying the method of homogenization and *at the same time* thin-domain approximation to such nano-structured layers. We investigate the resulting effective transmission condition and represent the cloaking problem as an optimization problem or a problem of exact controllability, the controls being shape, topology and material parameters for the inclusions constituting the microstructure.

In the context of mathematical modeling, there are many connections and analogies between acoustics and optics. Below we summarize some recent investigations on homogenization of periodically heterogeneous structures exposed to inciding acoustic, or electromagnetic waves. Namely the following issues are discussed:

- Phononic metamaterials which may exhibit negative effective mass for certain frequency ranges (the so called band-gaps).
- Homogenized 'acoustic sieve' problem; there the periodic perforation of a rigid layer (the obstacle) influences the acoustic impedance of the discontinuity interface.
- In analogy to the 'phononic' metamaterials, the 'photonic' ones may provide frequency-dependent magnetic permeability which may become even negative for some frequencies.

- As a central theme of this contribution is related to the cloaking problem, we discus the optical transmission on thin heterogeneous surface. The homogenization of such structure leads to a model resembling the homogenized acoustic sieve problem.

In all of the above cases combinations of 'classical' materials and geometrical arrangement of the heterogeneities gives rise to 'new' materials – *metamaterials* – characterized by their *effective properties* which makes their behaviour qualitatively different from any of the individual components. Especially the geometrical influence of materials' microstructures is challenging and inspires the *metamaterial optimal design*. We consider the cloaking problem formulated as the optimization problem parametrized by the *homogenized* metamaterial structure, i.e. by geometry of the heterogeneities distributed in the cloaking layer.
The optimization problem will also be considered in the context finite diameter material inclusion, thus without homogenization. For the interlacing of optimization and optimization and optimal control see Kogut and Leugering [20, 21, 22, 23]

Topology optimization for the cloaking problem

Instead of transformation techniques and the method of optimizing micro-structures before or after homogenization one may look directly into material optimization of coated objects. Indeed, given a region to be cloaked by a layer with material inclusions or 'holes', one may want to use topology optimization and shape optimization in order to find such optimal 'micro-structures'. More precisely, the concept of material interpolation (SIMP) [5] can be used in order to detect material densities of a given class of materials around the object. Moreover, the concept of topological derivatives or topological sensitivities can be used to check as to whether at a given point in the cloaking region an inclusion should be considered. Once the location is detected a subsequent shape sensitivity analysis followed by shape variation will then assign the optimal shape of that inclusion. Variations of this theme will be discussed in this contribution.

HOMOGENIZATION FOR MODELING OF METAMATERIALS IN ACOUSTIC AND ELECTROMAGNETIC WAVE PROPAGATION

Homogenization of periodically heterogeneous structures is a well accepted mathematical tool which enables one to reduce significantly the complexity of modeling such structures. The complexity is due to "detailed geometry" associated with description of piecewise defined material coefficients (properties), which at the end may lead to an intractable numerical problem featured by millions of unknowns and huge data to be treated. "Averaging" of the material properties, based on the asymptotic analysis and the representative volume element (the representative periodic cell) leads to the "homogenized medium" described by the effective material parameters, so that the whole structure can be described with a few data.
In this section we demonstrate how the homogenization approach (see e.g. [1, 13, 14, 15, 41] for general references) can be used to approximate dispersion properties in strongly heterogeneous media. In the case of *phononic* and *photonic* materials, the dispersion (and thereby the possible occurrence of band gaps) is retained even in the homogenized medium, due to special scaling of material properties of one of the material components.

PHONONIC MATERIALS – ELASTIC AND PIEZOELECTRIC WAVES

We now consider an elastic medium formed by periodic structures involving very soft substructures. Thus, the material properties, being attributed to material constituents vary periodically with the local position. Throughout the text all the quantities varying with this microstructural periodicity are labeled with superscript $^\varepsilon$, where ε is the characteristic scale of the microstructure. Typically ε can be considered as the ratio between the microstructure size and the incident wave length.

Periodic strongly heterogeneous material

The material properties are associated to the periodic geometrical decomposition which is now introduced. We consider an open bounded domain $\Omega \subset \mathbb{R}^3$ and the reference (unit) cell $Y =]0,1[^3$ with an embedded inclusion $\overline{Y_2} \subset Y$, whereby the matrix part is $Y_1 = Y \setminus \overline{Y_2}$. Let us note, that Y may be defined as a parallelepiped, the particular choice of the unit cube is just for ease of explanation. Using the reference cell we generate the decomposition of Ω as the union of all inclusions (which should not penetrate $\partial\Omega$), having the size $\approx \varepsilon$,

$$\Omega_2^\varepsilon = \bigcup_{k \in \mathbb{K}^\varepsilon} \varepsilon(Y_2 + k) , \quad \text{where } \mathbb{K}^\varepsilon = \{k \in \mathbb{Z} | \; \varepsilon(k + \overline{Y_2}) \subset \Omega\} , \tag{16}$$

whereas the perforated matrix is $\Omega_1^\varepsilon = \Omega \setminus \Omega_2^\varepsilon$. Also we introduce the interface $\Gamma^\varepsilon = \overline{\Omega_1^\varepsilon} \cap \overline{\Omega_2^\varepsilon}$, so that $\Omega = \Omega_1^\varepsilon \cup \Omega_2^\varepsilon \cup \Gamma^\varepsilon$.

Properties of a three dimensional body made of the elastic material are described by the elasticity tensor c^ε_{ijkl}, where $i,j,k = 1,2,\dots,3$. As usually we assume both major and minor symmetries of c^ε_{ijkl} ($c^\varepsilon_{ijkl} = c^\varepsilon_{jikl} = c^\varepsilon_{klij}$).

We assume that inclusions are occupied by a "very soft material" in the sense that the coefficients of *the elasticity tensor in the inclusions* are significantly smaller than those of the matrix compartment, however *the material density* is comparable in both the compartments. Such structures exhibit remarkable band gaps. Here, as an important feature of the modeling based on asymptotic analysis, the ε^2 scaling of elasticity coefficients in the inclusions appears. This *strong heterogeneity* in elasticity coefficients is related to the geometrical scale of the underlying microstructure (possibly another composite material involving "soft" and "hard" materials). The following ansatz is considered:

$$\begin{aligned} \rho^\varepsilon(x) &= \begin{cases} \rho^1 & \text{in } \Omega_1^\varepsilon, \\ \rho^2 & \text{in } \Omega_2^\varepsilon, \end{cases} \\ c^\varepsilon_{ijkl}(x) &= \begin{cases} c^1_{ijkl} & \text{in } \Omega_1^\varepsilon, \\ \varepsilon^2 c^2_{ijkl} & \text{in } \Omega_2^\varepsilon. \end{cases} \end{aligned} \tag{17}$$

Extension for piezoelectric materials.

Properties of a three dimensional body made of the piezoelectric material are described by three tensors: the elasticity tensor c^ε_{ijkl}, the dielectric tensor d_{ij} and the piezoelectric coupling tensor g^ε_{kij}, where $i,j,k = 1,2,\dots,3$. The following additional symmetries hold: $d^\varepsilon_{ij} = d^\varepsilon_{ji}$ and $g^\varepsilon_{kij} = g^\varepsilon_{kji}$.

In analogy with the purely elastic case, the scaling of material coefficients by ε^2 is considered in Ω_2^ε, except of the density:

$$\begin{aligned} \rho^\varepsilon(x) &= \begin{cases} \rho^1 & \text{in } \Omega_1^\varepsilon, \\ \rho^2 & \text{in } \Omega_2^\varepsilon, \end{cases} \\ c^\varepsilon_{ijkl}(x) &= \begin{cases} c^1_{ijkl} & \text{in } \Omega_1^\varepsilon, \\ \varepsilon^2 c^2_{ijkl} & \text{in } \Omega_2^\varepsilon, \end{cases} \\ g^\varepsilon_{kij}(x) &= \begin{cases} g^1_{kij} & \text{in } \Omega_1^\varepsilon, \\ \varepsilon^2 g^2_{kij} & \text{in } \Omega_2^\varepsilon, \end{cases} \\ d^\varepsilon_{ij}(x) &= \begin{cases} d^1_{ij} & \text{in } \Omega_1^\varepsilon, \\ \varepsilon^2 d^2_{ij} & \text{in } \Omega_2^\varepsilon. \end{cases} \end{aligned} \tag{18}$$

Modeling the stationary waves

We consider stationary wave propagation in the medium introduced above. Although the problem can be treated for a general case of boundary conditions, for simplicity we restrict the model to the description of clamped structures loaded by volume forces. Assuming a harmonic single-frequency volume forces,

$$\boldsymbol{F}(x,t) = \boldsymbol{f}(x) e^{i\omega t} , \tag{19}$$

where $\boldsymbol{f} = (f_i), i = 1,2,3$ is its local amplitude and ω is the frequency. We consider a dispersive displacement field with the local magnitude $\boldsymbol{u}^\varepsilon$

$$\boldsymbol{U}^\varepsilon(x,\omega,t) = \boldsymbol{u}^\varepsilon(x,\omega) e^{i\omega t} . \tag{20}$$

This allows us to study the steady periodic response of the medium, as characterized by displacement field $\boldsymbol{u}^\varepsilon$ which satisfies the following boundary value problem:

$$\begin{aligned} -\omega^2 \rho^\varepsilon \boldsymbol{u}^\varepsilon - \operatorname{div} \sigma^\varepsilon = \rho^\varepsilon \boldsymbol{f} \quad & \text{in } \Omega, \\ \boldsymbol{u}^\varepsilon = 0 \quad & \text{on } \partial\Omega, \end{aligned} \tag{21}$$

where the stress tensor $\sigma^\varepsilon = (\sigma^\varepsilon_{ij})$ is expressed in terms of the linearized strain tensor $\boldsymbol{e}^\varepsilon = (e^\varepsilon_{ij})$ by the Hooke's law $\sigma^\varepsilon_{ij} = c^\varepsilon_{ijkl} e_{kl}(\boldsymbol{u}^\varepsilon)$. Problem (21) can be formulated in a weak form as follows: Find $\boldsymbol{u}^\varepsilon \in \mathbf{H}^1_0(\Omega)$ such that

$$\begin{aligned} -\omega^2 \int_\Omega \rho^\varepsilon \boldsymbol{u}^\varepsilon \cdot \boldsymbol{v} + \int_\Omega c^\varepsilon_{ijkl} e_{kl}(\boldsymbol{u}^\varepsilon) e_{ij}(\boldsymbol{v}) = \\ = \int_\Omega \boldsymbol{f} \cdot \boldsymbol{v} \quad \text{for all } \boldsymbol{v} \in \mathbf{H}^1_0(\Omega) , \end{aligned} \tag{22}$$

where $\mathbf{H}^1_0(\Omega)$ is the standard Sobolev space of vectorial functions with square integrable generalized derivatives and with vanishing trace on $\partial\Omega$, as required by $(21)_2$. The weak problem formulation (22) is convenient for the asymptotic analysis using the two-scale convergence [1], or the unfolding method of homogenization [13].

Extension for piezoelectric materials. In addition, a synchronous harmonic excitation by volume charges with a single frequency ω can be considered $\tilde{q}(x,t) = q(x) e^{i\omega t}$, where q is the magnitude of the distributed volume charge. Accordingly, we should expect a dispersive piezoelectric field with magnitudes $(\boldsymbol{u}^\varepsilon, \varphi^\varepsilon)$

$$\begin{aligned} \tilde{\boldsymbol{u}}^\varepsilon(x,\omega,t) &= \boldsymbol{u}^\varepsilon(x,\omega) e^{i\omega t} , \\ \tilde{\varphi}^\varepsilon(x,\omega,t) &= \varphi^\varepsilon(x,\omega) e^{i\omega t} . \end{aligned}$$

Then the periodic response of the medium is characterized by field $(\boldsymbol{u}^\varepsilon, \varphi^\varepsilon)$ which satisfies the following boundary value problem:

$$
\begin{aligned}
-\omega^2\rho^\varepsilon \boldsymbol{u}^\varepsilon - \mathrm{div}\boldsymbol{\sigma}^\varepsilon &= \rho^\varepsilon \boldsymbol{f} \quad \text{in } \Omega,\\
-\mathrm{div}\boldsymbol{D}^\varepsilon &= q \quad \text{in } \Omega,\\
\boldsymbol{u}^\varepsilon &= 0 \quad \text{on } \partial\Omega,\\
\varphi^\varepsilon &= 0 \quad \text{on } \partial\Omega,
\end{aligned}
\tag{23}
$$

where the stress tensor $\boldsymbol{\sigma}^\varepsilon = (\sigma^\varepsilon_{ij})$ and the electric displacement $\boldsymbol{D}^\varepsilon$ are defined by constitutive laws

$$
\begin{aligned}
\sigma^\varepsilon_{ij} &= c^\varepsilon_{ijkl} e_{kl}(\boldsymbol{u}^\varepsilon) - g^\varepsilon_{kij}\partial_k \varphi^\varepsilon,\\
D^\varepsilon_k &= g^\varepsilon_{kij} e_{kl}(\boldsymbol{u}^\varepsilon) + d^\varepsilon_{kl}\partial_l \varphi^\varepsilon.
\end{aligned}
\tag{24}
$$

The problem (23) can be weakly formulated as follows: Find $(\boldsymbol{u}^\varepsilon, \varphi^\varepsilon) \in \mathbf{H}^1_0(\Omega)\times H^1_0(\Omega)$ such that

$$
\begin{aligned}
-\omega^2\int_\Omega \rho^\varepsilon \boldsymbol{u}^\varepsilon\cdot\boldsymbol{v} + \int_\Omega c^\varepsilon_{ijkl} e_{kl}(\boldsymbol{u}^\varepsilon) e_{ij}(\boldsymbol{v}) - &\\
-\int_\Omega g^\varepsilon_{kij} e_{ij}(\boldsymbol{v})\partial_k \varphi^\varepsilon &= \int_\Omega \boldsymbol{f}\cdot\boldsymbol{v}\,,\\
\int_\Omega g^\varepsilon_{kij} e_{ij}(\boldsymbol{u}^\varepsilon)\partial_k\psi + \int_\Omega d_{kl}\partial_l\varphi^\varepsilon\partial_k\psi &= \int_\Omega q\psi\,,
\end{aligned}
\tag{25}
$$

for all $(\boldsymbol{v},\psi) \in \mathbf{H}^1_0(\Omega)\times H^1_0(\Omega)$.

The homogenized model

Due to the *strong heterogeneity* in the elastic (and other piezoelectric) coefficients, the homogenized model exhibits dispersive behaviour; this phenomenon cannot be observed when standard two-scale homogenization procedure is applied to a medium without scale-dependent material parameters, as pointed out e.g. in [3]. In [4] the unfolding operator method of homogenization [13] was applied with the strong heterogeneity assumption (17), (18) We shall now record the resulting homogenized equations, as derived in [4], which describe the structure behaviour at the “macroscopic”scale. They involve the homogenized coefficients which depend on the characteristic responses at the “microscopic” scale.

Below it can be seen that the “frequency–dependent” mass coefficients are determined just by material properties of the inclusion and by the material density ρ^1 in the matrix, whereas the elasticity (and other piezoelectric) coefficients are related exclusively to the matrix material occupying the perforated domain.

For brevity in what follows we employ the following notations:

$$
\begin{aligned}
a_{Y_2}(\boldsymbol{u},\boldsymbol{v}) &= \int_{Y_2} c^2_{ijkl} e^y_{kl}(\boldsymbol{u})\, e^y_{ij}(\boldsymbol{v}),\\
d_{Y_2}(\phi,\psi) &= \int_{Y_2} d^2_{kl}\partial^y_l\phi\,\partial^y_k\psi,\\
g_{Y_2}(\boldsymbol{u},\psi) &= \int_{Y_2} g^2_{kij} e^y_{ij}(\boldsymbol{u})\,\partial^y_k\psi,\\
\rho_{Y_2}(\boldsymbol{u},\boldsymbol{v}) &= \int_{Y_2}\rho^2\boldsymbol{u}\cdot\boldsymbol{v},
\end{aligned}
\tag{26}
$$

whereby analogous notations are used when the integrations apply over Y_1.

Elastic medium. *Frequency–dependent homogenized mass* involved in the macroscopic momentum equation are expressed in terms of eigenelements $(\lambda^r, \boldsymbol{\varphi}^r) \in \mathbb{R}\times\mathbf{H}^1_0(Y_2),\ r = 1,2,\dots$ of the elastic spectral problem which is imposed in inclusion Y_2 with $\boldsymbol{\varphi}^r = 0$ on ∂Y_2:

$$
\begin{aligned}
\int_{Y_2} c^2_{ijkl} e^y_{kl}(\boldsymbol{\varphi}^r)\, e^y_{ij}(\boldsymbol{v}) = \lambda^r\int_{Y_2}\rho^2\boldsymbol{\varphi}^r\cdot\boldsymbol{v}\ \forall\boldsymbol{v}\in\mathbf{H}^1_0(Y_2)\,,\\
\int_{Y_2}\rho^2\boldsymbol{\varphi}^r\cdot\boldsymbol{\varphi}^s = \delta_{rs}\,.
\end{aligned}
\tag{27}
$$

To simplify the notation we introduce the *eigenmomentum* $\boldsymbol{m}^r = (m^r_i)$,

$$
\boldsymbol{m}^r = \int_{Y_2}\rho^2\boldsymbol{\varphi}^r. \tag{28}
$$

The effective mass of the homogenized medium is represented by mass tensor $\boldsymbol{M}^* = (M^*_{ij})$, which is evaluated as

$$
M^*_{ij}(\omega^2) = \frac{1}{|Y|}\int_Y \rho\,\delta_{ij} - \frac{1}{|Y|}\sum_{r\geq 1}\frac{\omega^2}{\omega^2-\lambda^r} m^r_i m^r_j\,; \tag{29}
$$

The elasticity coefficients are computed just using the same formula as for the perforated matrix domain, thus being independent of the inclusions material:

$$
C^*_{ijkl} = \frac{1}{|Y|}\int_{Y_1} c^1_{pqrs} e^y_{rs}(\boldsymbol{w}^{kl}+\Pi^{kl}) e_{pq}(\boldsymbol{w}^{ij}+\Pi^{ij})\,, \tag{30}
$$

where $\Pi^{kl} = (\Pi^{kl}_i) = (y_l\delta_{ik})$ and $\boldsymbol{w}^{kl}\in\mathbf{H}^1_\#(Y_1)$ are the corrector functions satisfying

$$
\int_{Y_1} c^1_{pqrs} e^y_{rs}(\boldsymbol{w}^{kl}+\Pi^{kl}) e^y_{pq}(\boldsymbol{v}) = 0 \quad \forall\boldsymbol{v}\in\mathbf{H}^1_\#(Y_1)\,. \tag{31}
$$

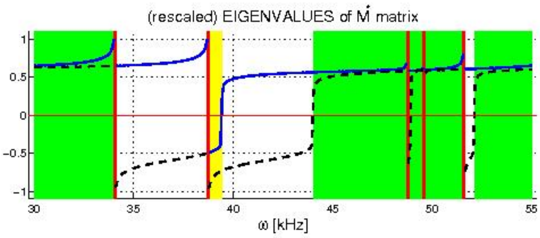

Fig. (1): Weak band gaps (white) and strong band gaps (yellow) computed for an elastic composite with L-shaped inclusions, the green bands are propagation zones.

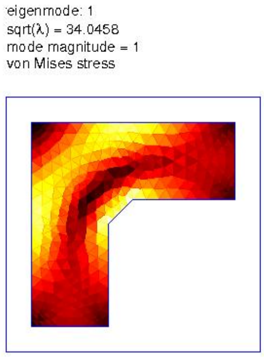

Fig. (2): The first eigenmode of the L-shaped clamped elastic inclusion.

Above $\mathbf{H}^1_\#(Y_1)$ is the restriction of $\mathbf{H}^1(Y_1)$ to the Y-periodic functions (periodicity w.r.t. the homologous points on the opposite edges of ∂Y).

The *global (homogenized) equation* of the homogenized medium, here presented in its differential form, describes the macroscopic displacement field $\boldsymbol{u}$:

$$\omega^2 M^*_{ij}(\omega) u_j + \frac{\partial}{\partial x_j} C^*_{ijkl} e_{kl}(\boldsymbol{u}) = -M^*_{ij}(\omega) f_j \,, \tag{32}$$

Heterogeneous structures with finite scale of heterogeneities exhibit the frequency *band gaps* for certain frequency bands. In the *homogenized medium*, the wave propagation depends on the positivity of mass tensor $\boldsymbol{M}^*(\omega)$; this effect is explained below.

Piezoelectric medium. In the piezoelectric medium, the spectral problem analogous to (27) comprises the additional constraint arising from electric charge conservation $(23)_2$: find eigenelements $[\lambda^r; (\varphi^r, p^r)]$, where $\varphi^r \in \mathbf{H}^1_0(Y_2)$ and $p^r \in H^1_0(Y_2)$, $r = 1, 2, \ldots$, such that

$$\begin{aligned} a_{Y_2}(\varphi^r, \boldsymbol{v}) - g_{Y_2}(\boldsymbol{v}, p^r) &= \lambda^r \rho_{Y_2}(\varphi^r, \boldsymbol{v}) \\ &\quad \forall \boldsymbol{v} \in \mathbf{H}^1_0(Y_2), \\ g_{Y_2}(\varphi^r, \psi) + d_{Y_2}(p^r, \psi) = 0 &\quad \forall \psi \in H^1_0(Y_2), \end{aligned} \tag{33}$$

with the orthonormality condition imposed on eigenfunctions φ^r:

$$a_{Y_2}(\varphi^r, \varphi^s) + d_{Y_2}(p^r, p^s) = \lambda^r \rho_{Y_2}(\varphi^r, \varphi^s) \stackrel{!}{=} \lambda^r \delta_{rs}. \tag{34}$$

Moreover, if $q \not\equiv 0$ in $(23)_2$, then the following problem must be solved: find $\tilde{p} \in H^1_0(Y_2)$, the unique solution satisfying

$$d_{Y_2}(\tilde{p}, \psi) = \int_{Y_2} \psi \qquad \forall \psi \in H^1_0(Y_2) \,. \tag{35}$$

The homogenized mass $M^*_{ij}(\omega)$ is evaluated using the same formula (29), as in the elastic case. Further new coefficients $Q^*_i(\omega)$ are introduced using the solution of (35)

$$Q^*_i(\omega) = -\frac{1}{|Y|} \sum_{r \geq 1} \frac{\omega^2}{\omega^2 - \lambda^r} m^r_i g_{Y_2}(\varphi^r, \tilde{p}), \tag{36}$$

describing influence of the volume charge on the mechanical loading.

The *piezoelectric coefficients* of the homogenized medium are defined in terms of the corrector basis functions satisfying the microscopic auxiliary problems:

1. Find $(\chi^{ij}, \pi^{ij}) \in \mathbf{H}^1_\#(Y_1) \times H^1_\#(Y_1)$, $i, j = 1, \ldots, 3$ such that (the notation corresponds to that introduced in (26))

$$\left\{ \begin{aligned} a_{Y_1}\left(\chi^{ij} + \Pi^{ij}, \boldsymbol{v}\right) - g_{Y_1}\left(\boldsymbol{v}, \pi^{ij}\right) &= 0 \,, \\ g_{Y_1}\left(\chi^{ij} + \Pi^{ij}, \psi\right) + d_{Y_1}\left(\pi^{ij}, \psi\right) &= 0 \,, \end{aligned} \right. \\ \forall \boldsymbol{v} \in \mathbf{H}^1_\#(Y_1), \forall \psi \in H^1_\#(Y_1) \,, \tag{37}$$

   where $\Pi^{ij} = (\Pi^{ij}_k) = (y_j \delta_{ik})$;

2. Find $(\chi^k, \pi^k) \in \mathbf{H}^1_\#(Y_1) \times H^1_\#(Y_1)$, $i, j = 1, \ldots, 3$ such that

$$\left\{ \begin{aligned} a_{Y_1}\left(\chi^k, \boldsymbol{v}\right) - g_{Y_1}\left(\boldsymbol{v}, \pi^k + \Pi^k\right) &= 0 \,, \\ g_{Y_1}\left(\chi^k, \psi\right) + d_{Y_1}\left(\pi^k + \Pi^k, \psi\right) &= 0 \,, \end{aligned} \right. \\ \forall \boldsymbol{v} \in \mathbf{H}^1_\#(Y_1), \forall \psi \in H^1_\#(Y_1) \,, \tag{38}$$

   where $\Pi^k = y_k$.

Using the corrector basis functions just defined the homogenized coefficients are expressed, as follows:

$$
\begin{aligned}
C^*_{ijkl} &= \frac{1}{|Y|} a_{Y_1}\left(\chi^{kl} + \Pi^{kl}, \chi^{ij} + \Pi^{ij}\right) + \\
&\quad + \frac{1}{|Y|} d_{Y_1}\left(\pi^{kl}, \pi^{ij}\right) , \\
D^*_{ki} &= \frac{1}{|Y|}\left[d_{Y_1}\left(\pi^k + \Pi^k, \pi^i + \Pi^i\right) + a_{Y_1}\left(\chi^k, \chi^i\right)\right] , \\
G^*_{kij} &= \frac{1}{|Y|}\left[g_{Y_1}\left(\chi^{ij} + \Pi^{ij}, \Pi^k\right) + d_{Y_1}\left(\pi^{ij}, \Pi^k\right)\right] .
\end{aligned}
\tag{39}
$$

The *global equation* describes the macroscopic field of displacements $\boldsymbol{u}$ and of electric potential φ

$$
\begin{aligned}
\omega^2 M^*_{ij}(\omega) u_j + \frac{\partial}{\partial x_j}\left(C^*_{ijkl} e_{kl}(\boldsymbol{u}) - G^*_{kij}\partial_k \varphi\right) &= \\
= -M^*_{ij}(\omega) - Q^*_i(\omega) q &, \\
\frac{\partial}{\partial x_k}\left(G^*_{kij} e_{ij}(\boldsymbol{u}) + D^*_{kl}\partial_l \varphi\right) = q &.
\end{aligned}
\tag{40}
$$

Further related work on the sensitivity analysis can be found in [32, 34].

Band gap prediction

As the main advantage of the homogenized models (32) and (40), by analyzing the dependence $\omega \to \boldsymbol{M}^*(\omega)$ one can determine distribution of the band gaps; it was proved in [4] that there exist frequency intervals G^k, $k = 1, 2, \ldots$ such that for $\omega \in G^k \subset]\lambda^k, \lambda^{k+1}[$ at least one eigenvalue of tensor $M^*_{ij}(\omega)$ is negative. Those intervals where all eigenvalues of M^*_{ij} are negative are called *strong*, or *full* band gaps. In the latter case the negative sign of the mass changes the hyperbolic type of the wave equation to the elliptic one, therefore any waves cannot propagate. In the "weak" bad gap situation only waves with certain polarization can propagate, as explained below.

The band gaps can be classified w.r.t. the polarization of waves which cannot propagate; the polarization is determined in terms of the eigenvectors of $M^*_{ij}(\omega)$. Given a frequency ω, there are three cases to be distinguished according to the signs of eigenvalues $\gamma^r(\omega)$, $r = 1, 2, 3$ (in 3D), which determines the "positivity, or negativity" of the mass:

1. **propagation zone** – All eigenvalues of $M^*_{ij}(\omega)$ are positive: then homogenized model (32), or (40) admits wave propagation without any restriction of the wave polarization;
2. **strong band gap** – All eigenvalues of $M^*_{ij}(\omega)$ are negative: then homogenized model (32), or (40) does *not* admit any wave propagation;
3. **weak band gap** – Tensor $M^*_{ij}(\omega)$ is indefinite, i.e. there is at least one negative and one positive eigenvalue: then propagation is possible only for waves polarized in a manifold determined by eigenvectors associated with positive eigenvalues. In this case the notion of wave propagation has a local character, since the "desired wave polarization" may depend on the local position in Ω.

In Fig. (1) we introduce a graphical illustration of the band gaps analyzed for an *elastic* material with L-shaped inclusions (its eigenmode fig. (2)). Whenever inclusions (considered in 2D) are symmetric w.r.t. more than 1 axis of symmetry, only strong band gaps exist, see Fig. (3). This may not be the case for *piezoelectric materials*; in Fig. (4) we illustrate dispersion curves and the weak band gaps obtained for a homogenized piezoelectric composite with circular inclusions.

Usually the band gaps are identified from the *dispersion* diagrams. For the homogenized model the dispersion of guided plane waves is analyzed in the standard way, using the following ansatz:

$$
\begin{aligned}
\boldsymbol{u}(x,t) &= \bar{\boldsymbol{u}}\, e^{-\mathrm{j}(\omega t - x_j \kappa_j)} , \\
\varphi(x,t) &= \bar{\varphi}\, e^{-\mathrm{j}(\omega t - x_j \kappa_j)} ,
\end{aligned}
\tag{41}
$$

where $\bar{\boldsymbol{u}}$ is the displacement polarization vector (the wave amplitude), $\bar{\varphi}$ is the electric potential amplitude, $\kappa_j = n_j \varkappa$, $|\boldsymbol{n}| = 1$, i.e. $\boldsymbol{n}$ is the incidence direction, and $\varkappa$ is the wave number. The dispersion analysis consists in computing nonlinear dependencies $\bar{\boldsymbol{u}} = \bar{\boldsymbol{u}}(\omega)$ and $\varkappa = \varkappa(\omega)$. For this one substitutes (41) into the homogenized model (40); on introducing projections of the homogenized tensors into the direction of the wave propagation,

$$
\Gamma_{ik} = C^*_{ijkl} n_j n_l \,, \; \gamma_i = G^*_{kij} n_j n_k \,, \; \zeta = D^*_{kl} n_l n_k \,, \tag{42}
$$

and substituting in (40), we obtain

$$
\begin{aligned}
-\omega^2 M^*_{ij}(\omega^2)\bar{u}_j + \varkappa^2\left(\Gamma_{ik}\bar{u}_k - \gamma_i \bar{\varphi}\right) &= 0 , \\
\varkappa^2\left(\gamma_k \bar{u}_k + \zeta \bar{\varphi}\right) &= 0 .
\end{aligned}
\tag{43}
$$

In (43) we can eliminate $\bar{\varphi}$ (assuming $\varkappa^2 \neq 0$), thus the dispersion analysis reduces to the "standard elastic case" where the acoustic tensor is modified, thus

$$
\begin{aligned}
-\omega^2 M^*_{ij}(\omega^2)\bar{u}_j + \varkappa^2 H_{ik}\bar{u}_k &= 0 , \\
\text{where} \quad H_{ik} = \Gamma_{ik} + \gamma_i \gamma_k / \zeta &
\end{aligned}
\tag{44}
$$

is analyzed as follows

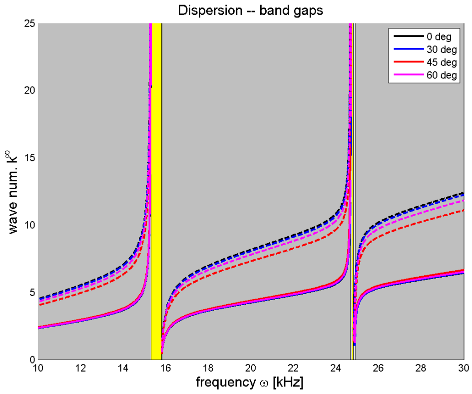

Fig. (3): Dispersion curves for guided waves in composites with circular inclusions: elastic material, only strong band gaps. Different angles of wave incidence displayed by different colours.

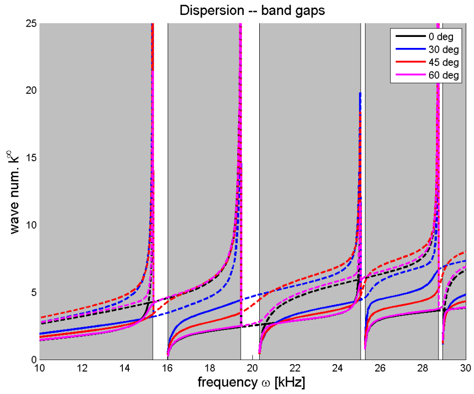

Fig. (4): Dispersion curves for piezoelectric material.

- for all $\omega \in [\omega^a, \omega^b]$ and $\omega \notin \{\lambda^r\}_r$ compute eigenelements $(\eta^\beta, \boldsymbol{w}^\beta)$:

$$\omega^2 M^*_{ij}(\omega^2) w^\beta_j = \eta^\beta H_{ik} w^\beta_k \;, \quad \beta = 1,2,3 \;; \tag{45}$$

- if $\eta^\beta > 0$, then $\varkappa^\beta = \sqrt{\eta^\beta}$,
- else ω falls in an *acoustic gap*, wave number is not defined.

In heterogeneous media *in general* the polarizations of the two waves (outside the band gaps) are *not mutually orthogonal*, which follows easily from the fact that $\{\boldsymbol{w}^\beta\}_\beta$ are $\boldsymbol{M}^*(\omega^2)$–orthogonal. Moreover, in the presence of the piezoelectric coupling, which introduces another source of anisotropy, the standard orthogonality is lost even for heterogeneous materials with "symmetric inclusions" (circle,hexagon, etc.), in contrast with elastic structures where these designs preserve the standard orthogonality.
More details on the band gap properties and their relationship to the dispersion of guided waves were discussed in [35, 30, 10]. The sensitivity analysis for the optimization problem was discussed in [31, 32, 34, 33].

ACOUSTIC TRANSMISSION ON PERFORATED INTERFACES

In this section we present an example which illustrates, how homogenization can be employed to describe acoustic transmission between two halfspaces separated by an interface that establishes a microstructure. The detailed analysis was presented in [38].
We consider the acoustic medium occupying domain Ω^G which is subdivided by perforated plane Γ_0 in two disjoint subdomains Ω^+ and Ω^-, so that $\Omega^G = \Omega^+ \cup \Omega^- \cup \Gamma_0$, see Fig. (7). Denoting by p the acoustic pressure field in $\Omega^+ \cup \Omega^-$, in a case of no convection flow, the acoustic waves in Ω^G are described by the following equations (ω is the frequency of the incident wave),

$$\begin{aligned} c^2\nabla^2 p + \omega^2 p = 0 \quad & \text{in } \Omega^- \cup \Omega^+ \;, \\ + \text{ boundary conditions} \quad & \text{on } \partial\Omega^G \;, \end{aligned} \tag{46}$$

supplemented by the transmission conditions on interface Γ_0 — these present *the key issue of this section*. The boundary conditions on Γ_0 will be specified later on. Let p^+ and p^- be the traces of p on $\partial\Omega^+ \cap \Gamma_0$ and on $\partial\Omega^- \cap \Gamma_0$, respectively.
The standard treatment of the acoustic transmission on a sieve-like perforation Γ_0 results in the relationship between jump $p^+ - p^-$ and normal derivatives $\frac{\partial p^+}{\partial n^+} = -\frac{\partial p^-}{\partial n^-}$,

$$\begin{aligned} \frac{\partial p^+}{\partial n^+} &= -\mathrm{j}\frac{\omega\rho}{Z}(p^+ - p^-), \\ \frac{\partial p^-}{\partial n^-} &= -\mathrm{j}\frac{\omega\rho}{Z}(p^- - p^+) \;, \end{aligned} \tag{47}$$

where n^+ and n^- are the outward unit normals to Ω^+ and Ω^-, respectively, ω is the frequency, ρ is the density and Z is the *transmission impedance*. This quantity incorporates many physical aspects of the transmission, namely the geometry – the design of the perforation. In [38] a homogenized transmission

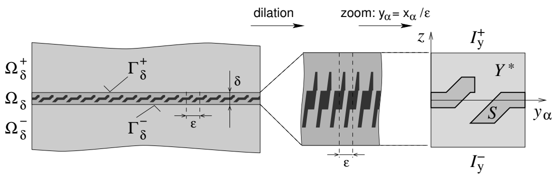

$$\Omega_\delta^\varepsilon \quad \overset{\text{dilatation}}{\longrightarrow} \quad \Omega^\varepsilon \quad \overset{\text{unfolding}}{\longrightarrow} \quad Y^*$$

Fig. (5): Left: global problem imposed in entire domain Ω^G before homogenization of the layer Ω_δ. Right: representative cell of the periodic structure. The dark patterns represent the obstacles in the fluid.

conditions were proposed which describe the acoustic impedance of the interface characterized by a periodically perforated obstacle embedded in a layer of thickness δ. In Figure (5) we illustrate such a layer Ω_δ embedded in $\Omega^G = \Omega_\delta^+ \cup \Omega_\delta^+ \cup \Omega_\delta \cup \Gamma_\delta^\pm$.

Periodic perforation and acoustic problem in the transmission layer

Let $\Gamma_0 \subset \mathbb{R}^2$ be an open bounded subdomain of the plane spanned by coordinates x_α, $\alpha = 1,2$ and containing the origin. Further let Γ_δ^+ and Γ_δ^- be equidistant to Γ_0 with the distance $\delta/2 = \mathrm{dist}(\Gamma_0, \Gamma_\delta^+) = \mathrm{dist}(\Gamma_0, \Gamma_\delta^-)$. We introduce *layer* $\Omega_\delta = \Gamma_0 \times]-\delta/2, \delta/2[\subset \mathbb{R}^3$, an open domain representing the transmission layer bounded by $\partial\Omega_\delta$ which is split as follows, see Fig. (6)

$$\begin{aligned}
\partial\Omega_\delta &= \Gamma_\delta^+ \cup \Gamma_\delta^- \cup \partial\Omega_\delta^\infty \,, \\
\Gamma_\delta^\pm &= \Gamma_0 \pm \frac{\delta}{2}\vec{e}_3 \,, \\
\partial\Omega_\delta^\infty &= \partial\Gamma_0 \times]-\delta/2, \delta/2[\,,
\end{aligned} \tag{48}$$

where $\delta > 0$ is the layer thickness and $\vec{e}_3 = (0,0,1)$, see Fig. (6). The acoustic medium occupies domain $\Omega_\delta^\varepsilon = \Omega_\delta \setminus \overline{S_\delta^\varepsilon}$, where S_δ^ε is the solid *rigid* obstacle which in a simple layout has a form of the periodically perforated sheet with the thickness $s\delta$, $s < 1$ and with ε characterizing the scale of the periodic perforation; thus, S_δ^ε is obtained by the usual *periodic lattice* extension of the solid unit structure. For passing to the limit $\varepsilon \to 0$ we consider a proportional scaling between the period length and the thickness, so that $\delta = h\varepsilon$, where $h > 0$ is fixed.

Acoustic problem in the layer. We assume a monochromatic wave propagation in layer Ω^δ. The total acoustic pressure, $p^{\varepsilon\delta}$ satisfies the Helmholtz

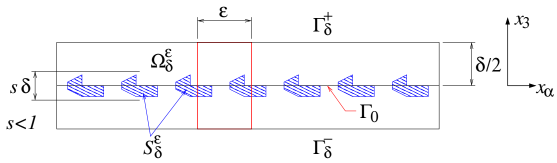

Fig. (6): Layer Ω_δ embedding the rigid obstacles periodically distributed. Obstacles should not approach the fictitious boundaries $\Gamma_\delta^\pm$, thus $s << 1$.

equation in $\Omega_\delta^\varepsilon$ and Neumann condition on $\partial\Omega_\delta$

$$\begin{aligned}
c^2\nabla^2 p^{\varepsilon\delta} + \omega^2 p^{\varepsilon\delta} &= 0 \quad \text{in } \Omega_\delta^\varepsilon \,, \\
c^2\frac{\partial p^{\varepsilon\delta}}{\partial n^\delta} &= -\mathrm{j}\omega g^{\varepsilon\delta\pm} \quad \text{on } \Gamma_\delta^\pm \,, \\
\frac{\partial p^{\varepsilon\delta}}{\partial n^\delta} &= 0 \quad \text{on } \partial S_\delta^\varepsilon \cup \partial\Omega_\delta^\infty \,,
\end{aligned} \tag{49}$$

where $c = \omega/\kappa$ is the speed of sound propagation and by n^δ we denote the normal vector outward to Ω_δ.

Homogenized transmission conditions

The asymptotic analysis of system (49) results in an equation which describes an acoustic wave propagating in the layer as a response to the incident wave acoustic momentum $g^{\varepsilon\pm}$. The following assumption is important.
Let us introduce *shifted* fluxes $\hat{g}^{\varepsilon\pm} \in L^2(\Gamma_0)$ such that $\hat{g}^{\varepsilon\pm}(\bar{x}) = g^{\varepsilon\pm}(x^\pm)$ where $x^\pm \in \Gamma^\pm$ are homologous points associated to $\bar{x} \in \Gamma_0$, i.e. $\bar{x} = (\bar{x}_\alpha, 0)$ and $x^\pm - \bar{x} = (0,0,\pm 1/2)$. We assume

$$\hat{g}^{\varepsilon\pm} \rightharpoonup g^{0\pm} \quad \text{weakly in } L^2(\Gamma_0) \,, \tag{50}$$

$$\frac{1}{\varepsilon}\left(\hat{g}^{\varepsilon+} + \hat{g}^{\varepsilon-}\right) \rightharpoonup 0 \quad \text{weakly in } L^2(\Gamma_0) \,, \tag{51}$$

consequently $g^0 \equiv g^{0+} = -g^{0-}$. This equality means continuity of the normal momentum, which is consistent with the consequence of (47).
The homogenized coefficients governing the acoustic transmission are introduced below using so called corrector functions defined in the reference periodic cell $Y =]0,1[^2 \times]-1/2,+1/2[\subset \mathbb{R}^3$. The acoustic medium occupies the domain $Y^* = Y \setminus S$, where $S \subset Y$ is the solid (rigid) obstacle. For clarity we use notation $I_y =]0,1[^2$ and $I_z =]-1/2,+1/2[$. The upper and lower boundaries are translations of $(I_y, 0)$; we define $I_y^+ = \{y \in \partial Y : z = 1/2\}$ and $I_y^- = \{y \in \partial Y : z = -1/2\}$. By $H^1_{\#(1,2)}(Y)$ we denote the space of $H^1(Y)$ functions which are “1-periodic”

in coordinates y_α, $\alpha = 1,2$; in this paper such functions will be called "transversely Y-periodic".

In [38] the homogenization of problem (49) was considered in detail. As the result, the homogenized transmission conditions were obtained, being expressed in terms of the *interface mean acoustic pressure* $p^0 \in H^1(\Gamma_0)$, and the *fictitious acoustic transverse velocity* $g^0 \in L^2(\Gamma_0)$; these quantities satisfy the following PDE system in weak form:

$$\begin{aligned}
\int_{\Gamma_0} A_{\alpha\beta}\partial^x_\beta p^0 \partial^x_\alpha q - f^*\omega^2 \int_{\Gamma_0} p^0 q + \mathrm{j}\omega \int_{\Gamma_0} B_\alpha \partial^x_\alpha q\, g^0 = 0\,,\\
-\mathrm{j}\omega \int_{\Gamma_0} D_\beta \partial^x_\beta p^0 \psi + \omega^2 \int_{\Gamma_0} F g^0 \psi = \\
-\mathrm{j}\omega \frac{1}{\varepsilon_0} \int_{\Gamma_0} (p^+ - p^-)\psi\,,
\end{aligned} \tag{52}$$

for all $q \in H^1(\Gamma_0)$ and $\psi \in L^2(\Gamma_0)$, where $f^* = \frac{|Y^*|}{|Y|}$ is the porosity related to the layer thickness. We remark that while $(52)_1$ is the direct consequence of (49) for $\varepsilon \to 0$, additional constraint $(52)_2$ arises due to coupling the "outer acoustic problem" imposed in $\Omega^G \setminus \Omega_\delta$ with the one imposed in the layer. A quite analogous treatment is employed in the electromagnetic transmission problem described in Section . Equations (52) involve the homogenized coefficients $A_{\alpha\beta}, B_\alpha, D_\alpha$ and F expressed in terms of the local corrector functions π^β and ξ.

The homogenized coefficients, A,B,F are determined by the solution of the local corrector problems. To simplify the notation, we introduce

$$\begin{aligned}
\hat\nabla q &= (\partial^y_\alpha q, h^{-1}\partial_z q),\\
a^*_Y(\pi,\xi) &= \int_{Y^*} \hat\nabla\pi\cdot\hat\nabla\xi\\
&= \int_{Y^*}\left(\partial^y_\alpha\pi\partial^y_\alpha\xi + \frac{1}{h^2}\partial_z\pi\partial_z\xi\right)\,,\\
\gamma^\pm(\xi) &= \int_{I^+_y}\xi - \int_{I^-_y}\xi\,.
\end{aligned} \tag{53}$$

The two following local corrector problems are defined: Find $\pi^\beta, \xi \in H^1_{\#(1,2)}(Y)/\mathbb{R}$ such that

$$\begin{aligned}
a^*_Y\left(\pi^\beta + y_\beta, \phi\right) = 0\,,\ \forall\phi \in H^1_{\#(1,2)}(Y),\ \beta = 1,2\,,\\
a^*_Y(\xi,\phi) = -\frac{|Y|}{hc^2}\gamma^\pm(\phi)\,,\ \forall\phi \in H^1_{\#(1,2)}(Y)\,,
\end{aligned} \tag{54}$$

see Fig. (9) where function ξ is displayed for three different microstructures. The homogenized coefficients are expressed in terms of π^α and ξ, as follows:

$$\begin{aligned}
A_{\alpha\beta} &= \frac{c^2}{|Y|} a^*_Y\left(\pi^\beta + y^\beta, \pi^\alpha + y^\alpha\right)\,,\\
h^{-1}D_\alpha = B_\alpha &= \frac{c^2}{|Y|} a^*_Y(\xi, y_\alpha)\,,\\
F &= \frac{1}{|I_y|}\gamma^\pm(\xi)\,.
\end{aligned} \tag{55}$$

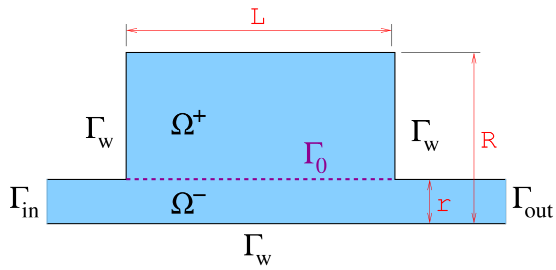

Fig. (7): The domain and boundary decomposition of the global acoustic problem considered. This layout is inspired by [8]

Structure of the global problem

The coupled system (52) described above constitute the transmission condition in a global problem considered. As an example, we shall present a model of an acoustic duct with perforated (rigid) plate.

Let us consider the domain of Ω^G, as in (46), where the outer boundary $\partial\Omega^G = \Gamma_{\rm in}\cup\Gamma_{\rm out}\cup\Gamma_{\rm w}$ consists of the planar surfaces $\Gamma_{\rm in}$, $\Gamma_{\rm out}$ and the channel walls $\Gamma_{\rm w}$, see Fig. (7). On $\Gamma_{\rm in}$ we assume an incident wave of the form $\tilde p(x,t) = \bar p e^{-\mathrm{j}kn_l\cdot x_l} e^{\mathrm{j}\omega t}$, where (n_l) is the outward normal vector of Ω, on $\Gamma_{\rm out}$ we impose the radiation condition of the Sommerfeld type, so that

$$\begin{aligned}
\mathrm{j}\omega p + c\frac{\partial p}{\partial n} &= 2\mathrm{j}\omega\bar p \quad \text{on } \Gamma_{\rm in}\,,\\
\mathrm{j}\omega p + c\frac{\partial p}{\partial n} &= 0 \quad \text{on } \Gamma_{\rm out}\,,\\
\frac{\partial p}{\partial n} &= 0 \quad \text{on } \Gamma_{\rm w}\,.
\end{aligned} \tag{56}$$

The interface condition has the following form, see illustration in Fig. (8),

$$\left\{\begin{aligned} c^2\frac{\partial p}{\partial n^+} &= \mathrm{j}\omega g_0\\ c^2\frac{\partial p}{\partial n^-} &= -\mathrm{j}\omega g_0\end{aligned}\right. \quad \text{on } \Gamma_0\,, \tag{57}$$

where $\frac{\partial p}{\partial n^\pm} = n^\pm\cdot\nabla p$ are the normal derivatives on Γ_0 w.r.t. normals outward to Ω^+ and Ω^-, respectively. Thus, transmission conditions on the interface Γ_0 involve the transversal acoustic momentum

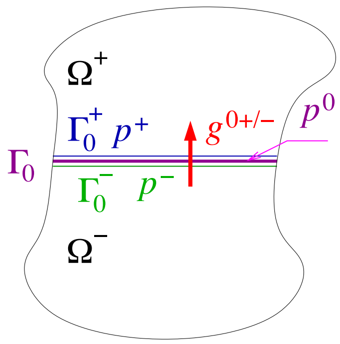

Fig. (8): Illustration of the transmission condition obtained by the homogenization of the perforated interface. Normal derivatives of the acoustic pressure are continuous, being proportional to g_0.

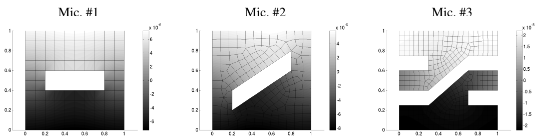

Fig. (9): Distribution of ξ in Y^*.

g_0 satisfying

$$
\begin{aligned}
-\partial_\alpha(A_{\alpha\beta}\partial_\beta p^0) + \omega^2 f^* p^0 - \partial_\alpha(B_\alpha g^0) = 0 \quad & \text{on } \Gamma_0 \,, \\
-\mathrm{j}h\omega B_\beta + \omega^2 F g^0 = -\mathrm{j}\omega \frac{1}{\varepsilon_0}(p^+ - p^-) \quad & \text{on } \Gamma_0 \,, \\
A_{\alpha\beta}\partial_\beta p^0 = 0 \quad & \text{on } \partial\Gamma_0 \,,
\end{aligned}
\tag{58}
$$

where $\partial\Gamma_0$ is the edge of the obstacle Γ_0 and $f^* = |Y^*|/|Y|$ is the layer porosity (depending on parameter h). This is the differential form of integral identities (52) that were developed in [38] using asymptotic analysis.

Numerical illustration

In Table 1 we introduce homogenized transmission parameters A, B, F for 2D microstructures #1, #2 and #3 displayed in Fig. (9); whenever the microstructure is symmetric w.r.t. the vertical axis of Y, coefficient B vanishes and, as the consequence, the surface wave is decoupled from the transversal momentum.

We shall now illustrate that the global macroscopic response is very sensitive to the specific geometry of the perforation. The following numerical example shows the global response of a waveguide containing the homogenized transmission layer. The geometry of the waveguide is depicted in Figs. (7). The

Mic.	$A[(\mathrm{m/s})^2]$	$B[\mathrm{m}]$	$F[\mathrm{s}^2]$
#1	$1.155 \cdot 10^5$	0	$1.391 \cdot 10^{-5}$
#2	$1.704 \cdot 10^5$	-0.251	$1.324 \cdot 10^{-5}$
#3	$2.186 \cdot 10^5$	-0.897	$4.265 \cdot 10^{-5}$

Table 1: Comparison of homogenized transmission parameters for different microstructures.

global response can be characterized by the transmission loss $TL = 20 log\left(|\bar{p}_{|\Gamma_{\rm in}}|/|p_{|\Gamma_{\rm out}}|\right)$, where $\bar{p}$ is the incident plane wave, see (56). The transmission losses for the waveguide with perforations #1, #2 and #3 are shown in Fig. (10). On the horizontal axis there is the wave number κ ($\kappa = \omega/c$) multiplied by length L of the "expansion chamber" (see Fig. (7)). The resulting acoustic pressures in the waveguide are displayed in Fig. (11). The numerical results were obtained for acoustic speed $c = 343\,\mathrm{m/s}$ and scale parameter $\varepsilon_0 = 0.035$, which e.g. for the microstructure type #1 means that the thickness of the perforated plate is 7mm. According to this study the perforation design seems to have quite important influence on the global behaviour of the acoustic pressure field, as viewed by the transmission losses. This is a motivation for an optimal perforation problem, see [29, 24].

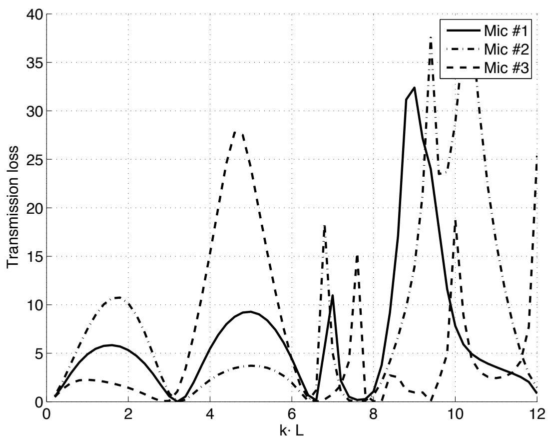

Fig. (10): Transmission losses for different perforation types.

ELECTROMAGNETIC WAVES IN PHOTONIC CRYSTALS

In analogy with the photonic crystals (materials) treated in Section , homogenization was employed to describe dispersion of optical waves in strongly heterogeneous periodic materials, cf.

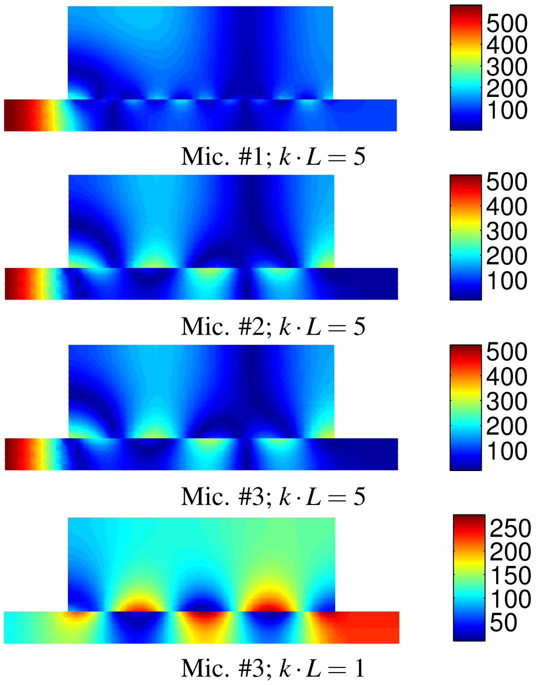

Fig. (11): Modulus of the acoustic pressure in Ω for $k \cdot L = 5$ (1 in the last picture). For this 2D computation a finite element mesh comprising 820 quadrilateral elements was used.

Helmholtz equation for harmonic waves

Here we recall the possible description of electromagnetic fields in heterogeneous materials using the Hertz potential (cf. [2]).

Maxwell equation for harmonic waves. We assume monochromatic wave of frequency ω and amplitudes $\boldsymbol{H}$ and $\boldsymbol{E}$ standing for magnetic and electric Fields, respectively, which satisfy the Maxwell equations:

$$\begin{aligned} \nabla \times \boldsymbol{H} &= (-\mathrm{j}\omega\varepsilon + \sigma)\boldsymbol{E} + \boldsymbol{J}_e \,, \\ \nabla \times \boldsymbol{E} &= \mathrm{j}\omega\mu \boldsymbol{H} \,, \\ \nabla \cdot (\varepsilon \boldsymbol{E}) &= \rho \,, \\ \nabla \cdot (\mu \boldsymbol{H}) &= 0 \,, \end{aligned} \tag{59}$$

where $\boldsymbol{J}_e$ is the current associated with external sources of electromagnetism, ρ is the volume electric charge density, ε is the electric permittivity (a real number), μ is the magnetic permeability (a real number) and σ is conductivity which is zero in vacuum (a real number).

Let us assume for a while, that the material is homogeneous, i.e. $(\varepsilon, \mu, \sigma)$ are constants. Then either $\boldsymbol{E}$, or $\boldsymbol{H}$ can be eliminated from system (59), so that the Helmholtz equations hold

$$\begin{aligned} \nabla^2 \boldsymbol{E} + \kappa^2 \boldsymbol{E} &= \varepsilon^{-1}\nabla\rho - \mathrm{j}\omega\mu \boldsymbol{J}_e \,, \quad \nabla \cdot \boldsymbol{E} = \rho/\varepsilon \,, \\ \nabla^2 \boldsymbol{H} + \kappa^2 \boldsymbol{H} &= -\nabla \times \boldsymbol{J}_e \,, \quad \nabla \cdot \boldsymbol{H} = 0 \,, \end{aligned} \tag{60}$$

where κ is the wave number characterized by the material:

$$\kappa^2 = \omega^2 \mu\beta = \omega^2 \mu(\varepsilon + \mathrm{j}\sigma/\omega) \,. \tag{61}$$

The vectorial Helmholtz equations (60) present three independent scalar “componentwise” equations, however they are coupled by the divergence conditions, which makes the analysis more difficult. To simplify construction of the solutions to (60), the *vector potentials* are introduced. Two standard cases can be treated:

1. **Electric Hertz potential.** Let us consider the special case $\boldsymbol{J}_e = 0$, thereby $\rho = 0$. Then by $(60)_1$ it follows that $\nabla \cdot \boldsymbol{E} = 0$. The electric Hertz potential $\boldsymbol{E} = \nabla \times \boldsymbol{A}^E$ then satisfies $(60)_1$, which yields
$$\nabla^2 \boldsymbol{A}^E + \kappa^2 \boldsymbol{A}^E = \nabla\phi \,, \tag{62}$$
where $\nabla\phi$ is any scalar differentiable function.
2. **Magnetic Hertz potential** of the magnetic field. Let $\boldsymbol{H} = \nabla \times \boldsymbol{A}^H$, where $\boldsymbol{A}^H$ is the Hertz potential. Then $(59)_2$ yields
$$\nabla^2 \boldsymbol{A}^H + \kappa^2 \boldsymbol{A}^H = -\boldsymbol{J}_e + \nabla\psi \,, \tag{63}$$
where ψ is any scalar differentiable function.

Transmission conditions. Let Γ be the interface separating two subdomains Ω_1 and Ω_2 where in each the material parameters are constant. From the integral form of the Maxwell equations the following transmission conditions can be derived, see e.g. [2],

$$[\boldsymbol{n} \times \boldsymbol{E}]_\Gamma = 0 \,, \quad [\boldsymbol{n} \times \boldsymbol{H}]_\Gamma = 0 \,, \tag{64}$$

where $[\bullet]_\Gamma$ is the jump of $\bullet$ on Γ and $\boldsymbol{n}$ is normal vector to Γ.

Two-dimensional model for a heterogeneous medium. Let us consider $\boldsymbol{A}^E = v\vec{e}_3$, so that $\vec{e}_3$ is the normal of the plane transversal to the fibres aligned with $\vec{e}_3$ and characterizing the heterogeneities, and $v = v(x_1, x_2)$ is the scalar potential of the transversal electric H-mode (TE-H-mode). Now (62) reduces to the scalar Helmholtz equation

$$\nabla^2 v + \kappa^2 v = \partial_3 \phi \,. \tag{65}$$

In what follows we may put $\nabla\phi = 0$, thus $\partial_3\phi = 0$, (cf. [2]). Further we consider two materials occupying two disjoint domains Ω_1 and Ω_2, separated by interface Γ, so that $\Omega = \Omega_1 \cup \Gamma \cup \Omega_2$. For this special case we rewrite $(64)_1$, noting that $\boldsymbol{n} \cdot \vec{e}_3 = 0$ and also $\vec{e}_3 \cdot (\nabla \boldsymbol{n}) = 0$:

$$\begin{aligned}
[\boldsymbol{n} \times \boldsymbol{E}]_\Gamma &= [\boldsymbol{n} \times \nabla \times \boldsymbol{A}^E]_\Gamma \\
&= [\nabla(\boldsymbol{n} \cdot \boldsymbol{A}^E) - (\nabla \boldsymbol{n}) \cdot \boldsymbol{A}^E - \partial_n \boldsymbol{A}^E]_\Gamma \\
&= -\vec{e}_3 [\partial_n v]_\Gamma ,
\end{aligned} \tag{66}$$

where ∂_n is the normal derivative. Then we employ $(59)_2$ in $(64)_2$:

$$\begin{aligned}
[\boldsymbol{n} \times \boldsymbol{H}]_\Gamma &= \frac{1}{\mathrm{j}\omega} [\frac{1}{\mu} \boldsymbol{n} \times \nabla \times \boldsymbol{E}]_\Gamma \\
&= \frac{-1}{\mathrm{j}\omega} [\frac{1}{\mu} \boldsymbol{n} \times \nabla^2 \boldsymbol{A}^E]_\Gamma \\
&= \vec{e}_3 \frac{-1}{\mathrm{j}\omega} [\frac{\kappa^2}{\mu} v]_\Gamma = 0 ,
\end{aligned} \tag{67}$$

where (64) was employed. Thus, for the time-harmonic response featured by the frequency ω and the TE-mode, the Maxwell equations yields the following system

$$\begin{aligned}
\nabla^2 v + \kappa^2 v = 0 \quad & \text{in } \Omega_k,\ k = 1,2 , \\
\text{some b.c. on } \partial\Omega , & \\
\text{transmission cond.:} \quad [\partial_n v]_\Gamma = 0 \quad & \text{on } \Gamma , \\
[\frac{\kappa^2}{\mu} v]_\Gamma = 0 \quad & \text{on } \Gamma ,
\end{aligned} \tag{68}$$

where ∂_n denotes the co-normal derivative, i.e. $\partial_n = \boldsymbol{n} \cdot \nabla$. The *complex wave number* κ is defined locally by the material parameters; we consider them piecewise constant in Ω, in particular

$$(\mu, \varepsilon, \sigma)(x) = \begin{cases} (\mu_1, \varepsilon_1, \sigma_1) & x \in \Omega_1 \\ (\mu_2, \varepsilon_2, \sigma_2) & x \in \Omega_2 \end{cases} , \tag{69}$$

where $(\mu_k, \varepsilon_k, \sigma_k)$, $k = 1,2$ are constants.
Meanwhile the boundary conditions on $\partial\Omega$ are not specified; importantly, when a part of $\partial\Omega$ is attached to a perfect conductor, then $\partial_n v = 0$ on this part.
It is worth noting that solutions to (68) have continuous co-normal derivative on Γ, but the traces of v on Γ are discontinuous. In the next section we modify the formulation represented by (68) to get rid of these discontinuities.
By virtue of the piecewise constant material properties (69) piecewise-defined rescaling of v restricted to Ω_k can be introduced. We shall see that there exists a continuous field u such that

$$v = \frac{\mu_k}{\kappa_k^2} u = \frac{1}{\varepsilon_k \omega^2 + \mathrm{j}\sigma_k \omega} u = \frac{1}{\omega^2 \beta_k} u \text{ in } \Omega_k \tag{70}$$

where $\beta_k = \varepsilon_k + \mathrm{j}\sigma_k/\omega$ and v satisfies (68). Substitution (70) is well defined provided $\omega > 0$ and $\varepsilon_k \neq 0$. Now we are allowed to apply this substitution in (68) to obtain the following modified system

$$\begin{aligned}
\nabla \cdot \left(\frac{1}{\beta_k} \nabla u \right) + \omega^2 \mu_k u = \partial_3 g \text{ in } \Omega_k,\ k = 1,2 , & \\
\text{some b.c. on } \partial\Omega , & \\
\text{transmission cond.: } [\frac{1}{\beta} \partial_n u]_\Gamma = 0 \quad \text{on } \Gamma , & \\
[u]_\Gamma = 0 \quad \text{on } \Gamma , &
\end{aligned} \tag{71}$$

where in $(71)_3$ $\beta = \beta_k$ on $\Gamma \cap \partial\Omega_k$. Obviously, continuity on Γ follows by $(71)_3$ and $(71)_4$ preserves continuity of the co-gradients.

Remark 1. Notation: Alternatively we can rewrite (71) using the relative permittivity and permeability. Let ε_0, μ_0 be the permittivity and permeability of the vacuum, then $\mu_k = \mu_k^r \mu_0$, $\varepsilon_k = \varepsilon_k^r \varepsilon_0$ and $\beta_k = \beta_k^r \varepsilon_0$, where $\beta_k^r(\omega) = \varepsilon_k^r + \mathrm{j}\sigma_k/(\omega\varepsilon_0)$. On introducing the wave number $\kappa_0 = \omega\sqrt{\varepsilon_0 \mu_0}$, $(71)_1$ can be rewritten (assuming $g = 0$)

$$\nabla \cdot \left(\frac{1}{\beta_k^r} \nabla u \right) + \kappa_0^2 \mu_k^r u = 0 \quad \text{in } \Omega_k,\ k = 1,2 . \tag{72}$$

For magnetically inactive materials $\mu_k^r \approx 1$, therefore alternatively

$$\nabla \cdot \left(\frac{1}{(n_k^r)^2} \nabla u \right) + \omega^2 \mu_0 u = 0 \quad \text{in } \Omega_k,\ k = 1,2 , \tag{73}$$

where $n_k^r = \sqrt{\beta_k^r/\varepsilon_0}$ is the refraction index.

△

Remark 2. Alternatively one can consider the so called transversal magnetic E-mode (TM-E-mode), on introducing $\boldsymbol{A}^H = w\vec{e}_3$, in analogy with the TE-H-mode. This applies in particular for $\boldsymbol{J}_e = j_e \vec{e}_3$, thus

$$\nabla^2 w + \kappa^2 w = -j_e + \partial_3 \psi .$$

The transmission conditions on Γ are

$$[\partial_n w]_\Gamma = 0, \quad [\mu w]_\Gamma = 0 ,$$

so that for μ constant in whole domain the solution w is smooth and continuous on Γ; typically this is satisfied by a class of optical materials where $\mu = \mu_0$.

$\triangle$

Photonic crystals

Photonic crystals and magnetically active materials became a quite interesting field of material science due to vast applications in optical technologies (waveguides, optical fibres, special lens...). There is a rich literature facing this subject, see e.g. [9][28][45].

In this section we aim to demonstrate the modelling analogy between acoustic waves in phononic materials and the electromagnetic waves in the photonic ones. Therefore, we shall focus on the homogenisation approach which consists in replacing a composite with a large number of periodic microstructures by a limit homogeneous material. Such a treatment is relevant for the modelling of the periodic structures presented by photonic crystals. As Bouchitté and Felbacq proposed [9] in the case of periodic photonic crystals made of "strongly heterogeneous composites" (i.e., with permittivity coefficients strongly different in the inclusions and in the matrix), the limit *homogenized permeability* is negative for certain wavelengths, thus yielding the existence of band gaps. More precisely, they showed that when the ratio between permeability of the inclusions and permeability of the background is of the order of the square of the size of the microstructures, then the band-gaps phenomenon appears. Historically this observation motivated the homogenization approach applied to elastic waves, as reported above.

Periodic structure with large contrasts in permittivity. Let us consider a periodic structure, as generated in (16), characterized by permeability $\mu^\varepsilon(x)$ and complex permittivity $\beta^\varepsilon(x)$ given as piecewise constant functions

$$
\begin{aligned}
\mu^\varepsilon(x) &= \begin{cases} \mu^1 & \text{in } \Omega_1^\varepsilon, \\ \mu^2 & \text{in } \Omega_2^\varepsilon, \\ \mu^0 & \text{in } \mathbb{R}^2 \setminus \Omega, \end{cases} \\
\beta^\varepsilon(x) &= \begin{cases} \beta^1 & \text{in } \Omega_1^\varepsilon, \\ \varepsilon^2\beta^2 & \text{in } \Omega_2^\varepsilon, \\ \beta^0 & \text{in } \mathbb{R}^2 \setminus \Omega \end{cases}
\end{aligned}
\tag{74}
$$

and assume that for $\varepsilon < \varepsilon_0$ no inclusion intersects $\partial\Omega$. Further we may assume that the heterogeneous medium occupying domain Ω is subject to an incident wave imposed in $\mathbb{R}^2 \setminus \Omega$ with the Sommerfeld radiation condition applied on the scattered field in the infinity, see [9]. Note that at any interface separating the inhomogeneities the standard interface condition of the type $(71)_3$ applies.

In [9] it was proved mathematically that the artificial magnetism can be obtained by homogenization (i.e. by asymptotic analysis) of the following problem

$$
\begin{aligned}
&\nabla \cdot \left(\frac{1}{\beta^\varepsilon} \nabla u^\varepsilon \right) + \omega^2 \mu^\varepsilon u^\varepsilon = 0 \quad \text{in } \mathbb{R}^2, \\
&\frac{1}{\beta^0} \partial_r u^{\mathrm{sc}\varepsilon} - \mathrm{j}\omega\mu^0 u^{\mathrm{sc}\varepsilon} = O(1/\sqrt{\kappa^0 r}) \\
&\qquad\qquad \text{when } r \to +\infty ,
\end{aligned}
\tag{75}
$$

where u^{inc} is the incident wave and $u^{\mathrm{sc}\varepsilon} = u^\varepsilon - u^{\mathrm{inc}}$ is the scattered field. We shall here recall the model of homogenized material (*metamaterial* which will allow us to see the analogies between the homogenization of the phononic crystals (acoustic waves) and the photonic ones (electromagnetic waves).

Homogenized coefficients. In analogy with the construction of mass tensor M^*_{ij} in (29) using eigensolutions of (27), the *effective permeability* is expressed in terms of eigensolutions of the problem: find couples $(\lambda^k, w^k) \in \mathbb{R} \times H^1_0(Y_2)$, $k = 1, 2, \ldots$

$$
\begin{aligned}
&\int_{Y_2} \nabla w^k \cdot \nabla \phi = \lambda^k \int_{Y_2} w^k \phi \ , \quad \forall \phi \in H^1_0(Y_2), \\
&\int_{Y_2} w^k w^l = \delta_{kl} \ .
\end{aligned}
\tag{76}
$$

Now the effective permeability is computed as follows:

$$
\begin{aligned}
\mu^*(\omega) = &\frac{\mu^1 |Y_1| + \mu^2 |Y_2|}{|Y|} + \\
&+ \mu^2 \frac{1}{|Y|} \sum_{k \in I_+} \frac{\omega^2}{\lambda^k/(\beta^2\mu^2) - \omega^2} \left(\int_{Y_2} w^k \right)^2 , \\
\text{where} \quad &I_+ = \{k| \quad \left| \int_{Y_2} w^k \right| > 0\} \ .
\end{aligned}
\tag{77}
$$

The *effective permittivity* becomes a 2×2 symmetric tensor:

$$
A^*_{ij} = \frac{1}{\beta^1} \fint_{Y_1} \nabla_y(\eta^i + y_i) \cdot \nabla_y(\eta^j + y_j) \ , \tag{78}
$$

where $\eta^i = H^1_\#(Y_1)$, being Y-periodic, satisfies the following identities:

$$
\fint_{Y_1} \nabla_y(\eta^i + y_i) \cdot \nabla_y \psi = 0 \quad \forall \psi \in H^1_\#(Y_1) \ , \quad i = 1, 2 \ ,. \tag{79}
$$

Homogenized photonic materials. The limit analysis of the heterogeneous medium leads to the model of homogenized medium which is characterized by effective (homogenized) material parameters. One can show that $u^\varepsilon(x)$ in (75) *two-scale converges* (cf. the unfolding method of homogenization [13]) to $u(x) + \chi_2(y)\hat{u}(x,y)$, where χ_2 is the characteristic function of Y_2 and $\hat{u}(x,y)$ are the non-vanishing oscillations in the inclusions. u is the "macroscopic" solution satisfying

$$
\begin{aligned}
\nabla_x \cdot \boldsymbol{A}^* \cdot \nabla_x u + \omega^2 \mu^*(\omega) u = 0 \,, &\quad \text{in } \Omega \,, \\
\frac{1}{\beta^0} \nabla^2 u + \omega^2 \mu^0 u = 0 \,, &\quad \text{in } \mathbb{R}^2 \setminus \Omega \,, \\
\boldsymbol{n} \cdot \boldsymbol{A}^* \cdot \nabla_x u_- - \boldsymbol{n} \cdot \frac{1}{\beta^0} \nabla u_+ = 0 &\quad \text{on } \partial\Omega \,, \\
u_+ - u_- = 0 &\quad \text{on } \partial\Omega \,, \\
u^{\rm sc} \equiv u - u^{\rm inc} &\quad \text{satisfies (75)} \,,
\end{aligned}
\tag{80}
$$

where $\boldsymbol{n}$ is a normal vector on $\partial\Omega$ and u_-, u_+ are the interior and exterior values on $\partial\Omega$, respectively. Thus the solution is continuous on $\partial\Omega$.

Photonic band gaps. The homogenized medium represented by $\mu^*(\omega)$ and A^*_{ij} is the magnetic active metamaterial with possibly negative permeability $\mu^*(\omega) < 0$ for some ω. This effect features occurrence of band gaps, in analogy with the *phononic* material described above in the text, where the acoustic band gaps are indicated by negative effective mass $M^*(\omega)$.

ELECTROMAGNETIC WAVE TRANSMISSION ON HETEROGENEOUS LAYERS AND CLOAKING

In analogy with the acoustic transmission problem reported in Section , we discus the electromagnetic wave transmission through periodically heterogeneous layer.

We consider a strip $\Omega_\delta \subset \mathbb{R}^3$ with the thickness $\delta > 0$ generated by a planar surface Γ_0 and bounded by Γ^+_δ and Γ^-_δ, see Fig. (12); the same notation is used as that introduced in Section . In general, the strip may contain perfect conducting material; we denote by $S^\varepsilon_\delta \subset \Omega^\varepsilon_\delta$ union of all such conductor (e.g. realized by fibrous graining) which also constitute the periodic pattern in the strip; length of the period in x_α, $\alpha = 1$ is ε, see Remark 3; the pattern is defined by the 2D section spanning coordinates x_1, x_3, so that interfaces of the graining between different materials have the form of general infinite cylinders. he dielectric material with finite conductivity occupies domain $\Omega^\varepsilon_\delta = \Omega_\delta \setminus \overline{S^\varepsilon_\delta}$. The problem of the TE-mode radiation will be imposed in the perforated domain $\Omega^\varepsilon_\delta$.

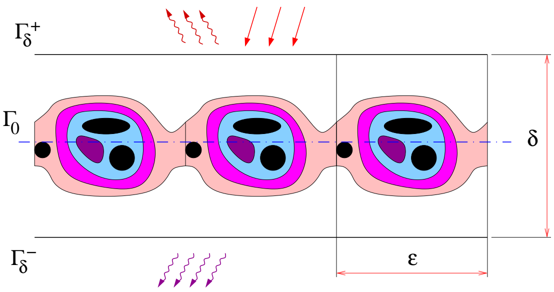

Fig. (12): Illustration of a section through the fictitious layer in which the heterogeneous structure is embedded. The black parts represent perfect conductors, in the "void" part the material coefficients are the same as those outside the layer; The colour (grey) regions are occupied by different materials.

Remark 3. Here we consider the TE-H-mode, i.e. the two-dimensional restriction of the electromagnetic wave propagation (65), which is characterized by scalar function $v = v(x_1, x_3)$, thus $\partial_2 v \equiv 0$. Such a situation is relevant whenever the heterogeneous structure is generated in 3D independently of coordinate x_2 (e.g. by fibrous graining aligned with x_2-axis). For generality we shall keep 3D description w.r.t. coordinates $(x_1, x_2, x_3) = (x_\alpha, x_3)$, where $\alpha = 1, 2$ refers to the in-plane position in Γ_0 only. However, due to the TE-H-mode restriction, only gradients w.r.t. x_1 and x_3 coordinates do not vanish, therefore in the sequel one may consider $\alpha = 1$.

In the "ad hoc 2D" treatment, Γ_0 is just a line, whereas Ω_δ is a two-dimensional domain spanned by coordinates x_1, x_3.

$\triangle$

From similar studies of elliptic problems in thin layers having a periodic microstructure it is well known that different limit models are obtained when commuting $\varepsilon \to 0$ (the period of heterogeneities) and $\delta \to 0$ (the thickness). Here we consider fixed proportion $\delta = h\varepsilon$, $h > 0$.

Non-homogenized layer – problem formulation

We can define the boundary value problem for the rescaled potential, see (71), and consider the Neumann conditions on $\Gamma_\delta^\pm$:

$$
\begin{aligned}
&\nabla\cdot\left(\frac{1}{\beta_{\varepsilon\delta}^2}\nabla u^{\varepsilon\delta}\right)+\mu\omega^2 u^{\varepsilon\delta}=0 \quad \text{in } \Omega_\delta^\varepsilon\,,\\
&\frac{1}{\beta_0}\partial_n^\pm u^{\varepsilon\delta}=\mathrm{j}\omega g^{\pm\delta} \quad \text{on } \Gamma_\delta^\pm\,,\\
&\text{where } g^{\pm\delta}=\pm g^0(x_\alpha)+\varepsilon g^{1\pm}(x_\alpha,x/\varepsilon)\,,\\
&\text{so that } \oint_{I_y^+\cup I_y^-} g^{\pm\delta}\approx\delta\,,\\
&\partial_n u^{\varepsilon\delta}=0 \quad \text{on } \partial S_\delta^\varepsilon\,,\\
&u^{\varepsilon\delta},\partial_n u^{\varepsilon\delta} \text{ periodic on opposite}\\
&\text{sides of } \partial\Omega_\delta^\infty\,,
\end{aligned}
\tag{81}
$$

where $g^{1\pm}$ is the fluctuation part. The perfect conductor in S_δ^ε results in the zero Neumann condition on the associated perforation boundary. It is worth recalling that $\beta_{\varepsilon\delta}$ is piecewise constant in $\Omega_\delta^\varepsilon$ and ε-periodic in x_1 (for fibrous structure relevant to the TE-mode analysis $\beta_{\varepsilon\delta}(x_1,x_3)$ is independent of x_2). In any case we assume that material on $\Gamma_\delta^\pm$ is homogeneous, thus $\beta_{\varepsilon\delta}=\beta_0$ is a *constant* (whatever possibly a complex number). Due to $(71)_{3,4}$ the solution $u^{\varepsilon\delta}$ is smooth and the transmission conditions are satisfied automatically.

Induction law constraint

For stating the boundary conditions on $\Gamma_\delta^\pm$, as explained below, the induction low is needed to define a suitable scaling of the Neumann fluxes.
Let $\mathscr{S}\in\mathbb{R}^2$ be a planar surface spanned by coordinates x_1,x_3, bounded by $\partial\mathscr{S}$, and let us consider decomposition $\mathscr{S}=\bigcup_k\mathscr{S}_k$ using a finite number of mutually non-overlapping subdomains $\mathscr{S}_k$, $k=1,2,\dots$; in each $\mathscr{S}_k$ the medium is assumed to be homogeneous. For zero external current, i.e. $\boldsymbol{J}_e=0$, and using the electric Hertz potential $\boldsymbol{A}^E$ the Maxwell equations $(59)_{1,2}$ yield $\boldsymbol{H}=(\sigma-\mathrm{j}\omega\varepsilon)\boldsymbol{A}^E$ and $\nabla\times\boldsymbol{E}=\mathrm{j}\omega\mu(\sigma-\mathrm{j}\omega\varepsilon)\boldsymbol{A}^E$ in each $\mathscr{S}_k$. Further let $\boldsymbol{t}^k$ be the tangent unit vector associated with closed oriented curve $\partial\mathscr{S}_k$ and let $\boldsymbol{E}^k$ be the trace on $\mathscr{S}_k$ of $\boldsymbol{E}$ defined in $\mathscr{S}_k$. On integrating in $\mathscr{S}_k$ and then using the summation over all subdomains, one obtains subsequently ($\mu^k,\varepsilon^k,\sigma^k$ are local material constants valid in $\mathscr{S}_k$):

$$
\begin{aligned}
&\bigcup_k\int_{\partial\mathscr{S}_k}\boldsymbol{t}^k\cdot\boldsymbol{E}^k d\Gamma=\bigcup_k\mu^k(\mathrm{j}\omega\sigma^k+\omega^2\varepsilon^k)\int_{\mathscr{S}_k}\boldsymbol{A}^E\,,\\
&\int_{\partial\mathscr{S}}\boldsymbol{t}\cdot\boldsymbol{E}d\Gamma=\int_{\mathscr{S}}\mu(\mathrm{j}\omega\sigma+\omega^2\varepsilon)\boldsymbol{A}^E\,.
\end{aligned}
\tag{82}
$$

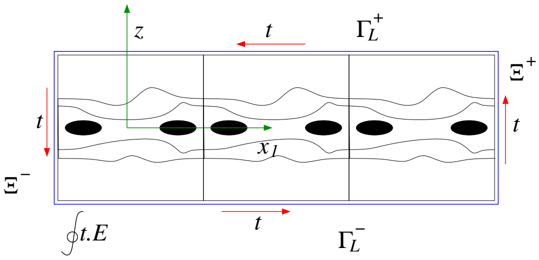

Fig. (13): Illustration of the integral form of the induction law.

Above the equivalence between the l.h.s. expressions follows from the general transmission condition (66) which in 2D situation of the TE-H-mode yields $[\boldsymbol{t}\cdot\boldsymbol{E}]_\Gamma=0$. Let $k\neq l$ and consider the integral over $\Gamma_{kl}=\partial\mathscr{S}_k\cap\partial\mathscr{S}_l$ which appears in the l.h.s. of $(82)_1$: due to the opposite curve orientation, $\boldsymbol{t}^k=-\boldsymbol{t}^l$ on Γ_{kl}, the following holds:

$$
\begin{aligned}
\int_{\partial\mathscr{S}_k\cap\Gamma_{kl}}\boldsymbol{t}^k\cdot\boldsymbol{E}^k d\Gamma+\int_{\partial\mathscr{S}_l\cap\Gamma_{kl}}\boldsymbol{t}^l\cdot\boldsymbol{E}^l d\Gamma=\\
=\int_{\Gamma_{kl}}[\boldsymbol{t}\cdot\boldsymbol{E}]_{\Gamma_{kl}}d\Gamma=0\,,
\end{aligned}
\tag{83}
$$

which yields the equivalence between the l.h.s. in $(82)_1$ and $(82)_2$.
In the 2D situation, due to the TE-mode assumption, (82) yields the following constraint

$$
\int_{\partial\mathscr{S}}(-t_1\partial_3 v+t_3\partial_1 v)d\Gamma=-\int_{\mathscr{S}}\kappa^2 v\,,
\tag{84}
$$

where $(t_1,0,t_3)$ is the tangent of $\partial\mathscr{S}$ and $v\vec{e}_2$ is the electric Hertz potential for the TE-mode. Note that (84) holds also on "perforated" domains $\mathscr{S}^*\subset\mathscr{S}$ when the perforation represents perfect conductors; this is the simple consequence of the homogeneous Neumann conditions on the part of $\partial\mathscr{S}^*$ attached to the conductors (the "holes").
We now consider $\Omega_\delta\supset\mathscr{S}=\Omega_{\delta L}=(\underline{x}+]-L/2,L/2[\,)\times]-\delta/2,\delta/2[$ where $\underline{x}\in\Gamma_0$ is such that $(\underline{x}+]-L/2,L/2[\,)\subset\Gamma_0$. Boundary of $\Omega_{\delta L}$ is as follows, see Fig. (13):

$$
\begin{aligned}
&\partial\Omega_{\delta L}=\Gamma_{\delta L}^+\cup\Gamma_{\delta L}^-\cup\Xi_\delta^-\cup\Xi_\delta^+\,,\\
&\Gamma_{\delta L}^\pm\subset\Gamma_\delta^\pm\,,\\
&\Xi_\delta^\pm=(\underline{x}\pm L/2)\times]-\delta/2,\delta/2[\,.
\end{aligned}
\tag{85}
$$

Using substitution (70) in (84) we obtain

$$
\frac{1}{\beta_0}\int_{\Gamma_{\delta L}^\pm}\partial_n^\pm u+\int_{\Xi_\delta^\pm}\frac{1}{\beta_{\varepsilon\delta}}\partial_n^\pm u=-\mu\omega^2\int_{\Omega_{\delta L}^{\varepsilon*}}u\,,
\tag{86}
$$

where $\Omega^{\varepsilon *}_{\delta L} = \Omega_{\delta L} \cap \Omega^{\varepsilon *}_{\delta}$ and where $\pm$ sign matches the integration over $\Gamma^{\pm}_{\delta L}$ or $\Xi^{\pm}_{\delta}$. It is important to note, that $|\Omega^{\varepsilon *}_{\delta L}|$ and $|\Xi^{\pm}_{\delta}|$ are proportional to δ; this observation was respected in the definition of $g^{\pm}_{\delta}$ in (81).

The homogenized transmission condition

The homogenized transmission condition is defined in terms of the homogenized coefficients which involve the corrector functions in the integral form. In what follows we explain, how the transmission condition can be evaluated, for its detailed derivation we refer to [37]. Here we shall just summarize the main steps of the homogenization procedure which is quite analogous to the result obtained for the acoustic problem reported above.

An important ingredient of the analysis is the dilation procedure, the affine mapping transforming domain Ω_δ on $\Omega = \Gamma_0 \times]-1/2, 1/2[$ which, thus, is independent of $\delta = h\varepsilon$. The material structure in the layer is periodic being generated by representative cell Y in analogy with the acoustic problem discussed in Section where the role of the fluid is now played by the dielectric material situated in Y^*, whereas the obstacles now represent the superconducting material.

Based on the *a priori estimate* of the solution to (81), one obtains the convergence result (in the sense of the two-scale convergence). There exist $u^0 \in L^2(\Gamma_0)$ and $u^1 \in L^2(\Gamma_0) \times H_{\#(1,2)}(Y)$ such that (denoting u^ε the solution of (81) on the dilated domain Ω) the following two-scale limits hold:

$$
\begin{aligned}
u^\varepsilon &\stackrel{2}{\rightarrow} u^0 \\
\partial_\alpha u^\varepsilon &\stackrel{2}{\rightarrow} \partial^x_\alpha u^0 + \partial^y_\alpha u^1 \,, \quad \alpha = 1,2 \\
\frac{1}{\varepsilon}\partial_z u^\varepsilon &\stackrel{2}{\rightarrow} \partial_z u^1
\end{aligned}
\tag{87}
$$

Below we introduce the corrector basis functions which enable to express the "microscopic" function u^1 in terms of the "macroscopic" quantities $\partial_\alpha u^0$ and g^0; these are involved in the homogenized Helmholtz equation arising from $(81)_1$.

Coupling the interface layer response with outer fields. In the limit situation the domain Ω_δ degenerates into the "mid-surface" (plane) Γ_0. Let the layer Ω_δ is embedded in Ω' where the scattered field can be observed,

$$
\Omega' = \Omega^+_\delta \cup \overline{\Omega_\delta} \cup \Omega^-_\delta \,, \quad \Omega^\pm_\delta \cap \Omega_\delta = \emptyset \,, \tag{88}
$$

where also Ω^+_δ and Ω^-_δ are disjoint. In order to be able to couple the exterior problem in $\Omega' \setminus \Omega_\delta$ with that in the homogenized layer represented by Γ, it is necessary to derive the relationship between the limit traces u^+ and u^- of the bulk field in $\Omega^\pm_\delta$ on $\Gamma^\pm$ for $\delta \to 0$ on one hand and the corresponding limit traces on $\Gamma^\pm_\delta$ on the other hand. Let $\widetilde{u^{\varepsilon\delta}}$ be the smooth extension over all perforations due to the perfect conductors. The traces from $\Omega^\pm_\delta$ satisfy

$$
\begin{aligned}
\int_{\Omega^\delta} \phi \partial_3 \widetilde{u^{\varepsilon\delta}} &= \int_{\Gamma^+_\delta} \phi\, u^\delta|_{\Gamma^+_\delta} d\Gamma - \int_{\Gamma^-_\delta} \phi\, u^\delta|_{\Gamma^-_\delta} d\Gamma \\
&\stackrel{\delta,\varepsilon\to 0}{\longrightarrow} \int_{\Gamma_0} \phi (u^+ - u^-) d\Gamma \,,
\end{aligned}
\tag{89}
$$

for any $\phi \in L^2(\Omega')$ constrained by $\partial_3 \phi = 0$. We shall now consider a finite thickness $\delta_0 > 0$ of the layer. The l.h.s. in (89) can also be written as $\delta_0 \int_\Omega \phi \partial_3 \widetilde{u^{\varepsilon_0\delta_0}}$ (we recall the use of smooth extension $\widetilde{u^{\varepsilon_0\delta_0}}$ to entire Ω_{δ_0}) . We consider the following approximation for $\varepsilon < \varepsilon_0$:

$$
\begin{aligned}
\delta_0 \int_\Omega \phi \partial_3 \widetilde{u^{\varepsilon_0\delta_0}} &\approx \varepsilon_0 \int_\Omega \frac{1}{\varepsilon} \phi \frac{\partial \widetilde{u^\varepsilon}}{\partial z} \\
&\stackrel{\varepsilon\to 0}{=\!=\!\longrightarrow} \varepsilon_0 \int_{\Gamma_0} \phi \fint_Y \left(\frac{\partial \widetilde{u^1}}{\partial z} \right) \\
&= \varepsilon_0 \int_{\Gamma_0} \phi \frac{1}{|I_y|} \left[\int_{I^+_y} u^1\, d\Gamma_y - \int_{I^-_y} u^1\, d\Gamma_y \right] \,,
\end{aligned}
\tag{90}
$$

for all $\phi \in L^2(\Gamma_0)$, see $(87)_3$, hence using (89)

$$
\int_{\Gamma_0} \phi (u^+ - u^-) d\Gamma = \varepsilon_0 \int_{\Gamma_0} \phi \frac{1}{|I_y|} \left[\int_{I^+_y} u^1\, d\Gamma_y - \int_{I^-_y} u^1\, d\Gamma_y \right] \,. \tag{91}
$$

Continuity or a jump of potential normal derivative on Γ_0? In the limit situation, $\varepsilon \to 0$, one can prove using the induction law constrain (86) that

$$
\frac{\partial u^+}{\partial n^+} + \frac{\partial u^-}{\partial n^-} = [\partial_n u]_{\Gamma_0} = 0 \,, \tag{92}
$$

where $\frac{\partial u^\pm}{\partial n^\pm}$ are traces from $\Omega^\pm$ of the normal derivatives on interface Γ_0.

However, an alternative treatment is possible. We may adapt the spirit of handling the potential jump $[u]_{\Gamma_0}$. For this we divide (86) by δ and approximate for a small $\delta_0 > 0$, which yields

$$
\frac{1}{\delta_0 \beta_0} \int_{\Gamma^\pm_L} \frac{\pm 1}{\delta} \frac{\partial}{\partial z} u + \int_{\Xi^\pm} \frac{\pm 1}{\beta_\varepsilon} \partial_1 u \approx -\mu\omega^2 \int_{\Omega^{\varepsilon *}_L} u \,. \tag{93}
$$

Above domains $\Gamma^\pm, \Xi^\pm, \Omega^{\varepsilon *}_L$ are obtained by the thickness dilatation (cf. [15],[38])of $\Gamma^\pm_\delta, \Xi^\pm_\delta, \Omega^{\varepsilon *}_{\delta L}$.

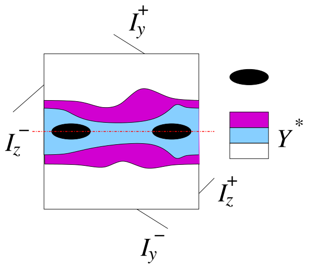

Fig. (14): Reference cell Y.

Since for $\varepsilon \to 0$ the second l.h.s. term vanishes, he limit of (93) results in

$$\frac{1}{\delta_0\beta_0}\left[\frac{\partial u^+}{\partial n^+}+\frac{\partial u^-}{\partial n^-}\right]=\frac{1}{\delta_0\beta_0}[\partial_n u]_{\Gamma_0}=-\rho^*\mu\omega^2u^0 \quad \text{for a.a. } x\in\Gamma_0\,, \tag{94}$$

where $\rho^* = |Y^*|/|Y|$.

Corrector basis functions. We employ notation introduced in Section , however now the bilinear form a_Y^* is modified:

$$a_Y^*(u,v)=\int_{Y^*}\frac{1}{\tilde\beta}\hat\nabla u\cdot\hat\nabla v\,dy\,, \tag{95}$$

where $\tilde\beta(y)$ is defined piecewise constant in Y^*. Due to linearity, we may define $\pi^\alpha,\xi\in H^1_\#(Y)$ such that

$$u^1=\pi^\alpha\partial^x_\alpha u^0+\mathrm{j}\omega\xi g^0\,, \tag{96}$$

and they satisfy the following auxiliary problems:

$$\begin{aligned} a_Y^*\left(\pi^\beta+y_\beta,\phi\right)&=0\,,\quad \forall\phi\in H^1_\#(Y)\,,\\ a_Y^*(\xi,\phi)&=\frac{1}{h}\gamma^\pm(\phi)\,,\quad \forall\phi\in H^1_\#(Y)\,. \end{aligned} \tag{97}$$

Macroscopic wave equation on Γ_0. The macroscopic equation governs the surface wave propagation. The limit of the Helmholtz equation reads as

$$\begin{aligned}\partial_\alpha A_{\alpha\beta}\partial_\beta u^0+\mathrm{j}\omega\partial_\alpha(B_\alpha g^0)+&\\ +\mu\omega^2\rho^*u^0&=\frac{\mathrm{j}\omega}{h}\sum_{s=+,-}\fint_{I_y^s}g^{1s}\end{aligned} \tag{98}$$

in Γ, where the homogenized coefficients are

$$\begin{aligned} A_{\alpha\beta}&=\frac{1}{|Y|}a_Y^*\left(\pi^\beta+y_\beta,\pi^\alpha+y_\alpha\right)\,,\\ B_\alpha&=\frac{1}{|Y|}a_Y^*(\xi,y_\alpha)\,. \end{aligned} \tag{99}$$

As the consequence of Remark 3, in fact $\alpha,\beta=1$ and A,B are only scalar values. Also $\partial_2 u^0=0$ due to the TE-H-mode restriction.

Jump condition. Using decomposition (96), from (90) for a.a. $x\in\Gamma_0$ we obtain

$$\begin{aligned} u^+-u^-&=\varepsilon_0\frac{1}{|I_y|}\gamma^\pm(u^1)\\ &=\varepsilon_0\frac{1}{|I_y|}\left(\gamma^\pm(\pi^\alpha)\partial^x_\alpha u^0+\mathrm{j}\omega\gamma^\pm(\xi)g^0\right)\\ &=\delta_0\left(-B_\alpha\partial^x_\alpha u^0+\mathrm{j}\omega F g^0\right)\,, \end{aligned} \tag{100}$$

where (note $|Y|=|I_z||I_y|$ and $|I_z|=1$)

$$F=\frac{1}{|Y|}a_Y^*(\xi,\xi)=\frac{1}{h|Y|\gamma^\pm(\xi)}\,. \tag{101}$$

Using auxiliary problems (97) one can verify that

$$\begin{aligned} a_Y^*(\xi,y_\alpha)&=-a_Y^*(\xi,\pi^\alpha)=-\frac{1}{h}\gamma^\pm(\pi^\alpha)\,,\\ \text{hence}\quad B_\alpha&=\frac{1}{|Y|}a_Y^*(\xi,y_\alpha)=-\frac{1}{h|I_y||Y_z|}\gamma^\pm(\pi^\alpha)\\ &=-\frac{1}{h|I_y|}\gamma^\pm(\pi^\alpha)\,, \end{aligned} \tag{102}$$

which was employed in (100).

Complete homogenized interface conditions. They involve the in-plane limit electric Hertz potential u^0 (see the transformation (70)), the transformed tangential electric field components, $g^+=g^0+\varepsilon_0 g^{1+}$ and $g^-=-g^0+\varepsilon_0 g^{1-}$ related to faces Γ^+ and Γ^-, respectively, where the fluctuating part is relevant for a given layer thickness $\delta_0=\varepsilon_0 h>0$. There is now discussion concerning the fluctuation parts $\varepsilon_0 g^{1s}$, $s=+,-$.

1. Let us consider the perfect continuity of normal derivatives according to (92). This is satisfied (in the sense of weak limits in $L^2(\Gamma_0)$) for the following two situations:
   a) for "the true limit case", $\varepsilon_0=0$, so that (92) holds for any $g^{1\pm}$ (since $\hat g^{\delta\pm}\rightharpoonup\pm g^0$ weakly in $L^2(\Gamma_0)$). In this case $g^{1\pm}$ is to be defined in (98).
   b) for the zero average in (98), i.e. assuming

   $$G^\pm\equiv\sum_{s=+,-}\fint_{I_y^s}g^{1s}=0\,. \tag{103}$$

   In this case functions $g^{1\pm}$ are not present in the limit model.

2. Let us now consider (94). Since the boundaries $\Gamma^{\pm}_{\delta}$ are not related to any structural (material) discontinuity, the normal derivatives must be continuous. Thus, for $\varepsilon_0 > 0$, the external field gradients represented by $\mathscr{T}_{\varepsilon}(g^+) = g^0(x_\alpha) + \varepsilon_0 g^{1+}(x_\alpha, y)$ are related to $\partial_n^{\pm} u^{\pm}$ by

$$\begin{aligned} \partial_n^+|_{\Gamma^+} u^+ &= \mathrm{j}\omega\beta_0^2 (g^0 + \varepsilon_0 \fint_{I_y^+} g^{1+}) , \\ \partial_n^-|_{\Gamma^-} u^- &= \mathrm{j}\omega\beta_0^2 (-g^0 + \varepsilon_0 \fint_{I_y^-} g^{1-}) , \end{aligned} \tag{104}$$

These "external field boundary conditions" can be substituted in (94), therefore

$$\begin{aligned} \frac{1}{\delta_0\beta_0^2}\left[\frac{\partial u^+}{\partial n^+} + \frac{\partial u^-}{\partial n^-}\right] &= \\ &= \frac{\mathrm{j}\omega}{\delta_0}\left(g^0 + \varepsilon_0 \fint_{I_y^+} g^{1+} - g^0 + \varepsilon_0 \fint_{I_y^-} g^{1-}\right) \\ &\stackrel{!}{=} -\rho^* \mu\omega^2 u^0 , \end{aligned} \tag{105}$$

hence the constraint

$$G^{\pm} \equiv \fint_{I_y^+} g^{1+} + \fint_{I_y^-} g^{1-} = \mathrm{j}\omega\rho^*\mu h u^0 \text{ a.e. on } \Gamma_0 . \tag{106}$$

We shall consider either (103) holds, so that the fluctuating parts are irrelevant in the limit situation, or (106) holds, which is an additional constraint. Therefore, the following problem is meaningful:
Let u^+ and u^- are given on faces Γ^+ and Γ^- of thin heterogeneous interface (with the thickness $\delta_0 << 1$) which is represented by surface (line in 2D – the relevant case) Γ_0 in the homogenized form. Denoting by $U_{\#}(\Gamma_0)$ the space of periodic functions on Γ_0, which is the consequence of periodic conditions $(81)_5$, we find $u^0 \in U_{\#}(\Gamma_0)$ and fluxes $g^0, G^{\pm} \in L^2(\Gamma_0)$ such that:

$$\begin{aligned} &\int_{\Gamma_0} A_{\alpha\beta}\partial^x_\beta u^0 \partial^x_\alpha v^0 + \mathrm{j}\omega\int_{\Gamma_0} B_\alpha g^0 \partial^x_\alpha v^0 - \\ &-\mu\omega^2\int_{\Gamma_0}\rho^* u^0 v^0 - \frac{\mathrm{j}\omega}{h}\int_{\Gamma_0} G^{\pm} v^0 = 0 \quad \forall v^0 \in U_{\#}(\Gamma_0) , \\ &\int_{\Gamma_0}\theta\left(-B_\alpha\partial^x_\alpha u^0 + \mathrm{j}\omega F g^0\right) = \frac{1}{\delta_0}\int_{\Gamma_0}\theta(u^+ - u^-) \\ &\qquad\qquad \forall\theta \in L^2(\Gamma_0) , \\ &G^{\pm} - \mathrm{j}\omega\zeta_0\rho^*\mu h u^0 = 0 \quad \text{a.e. on } \Gamma_0 , \end{aligned} \tag{107}$$

where $\zeta_0 = 0, 1$ in $(107)_3$, according to the case (103) and (106), respectively.

Cloaking problem

The cloaking problem consists in finding model parameters related to some subdomain $\Omega^- \subset \Omega^G$ such that an object $\Omega_c \subset \Omega^-$ is not visible outside Ω^-, i.e. the *incident wave* imposed in $\Omega^+ = \Omega^G \setminus \Omega^-$ is not perturbed by a refracted field on $\Gamma_s \subset \partial\Omega^G$. The medium parameters in Ω^G are defined as piecewise constant functions (pcw. const. func.):

domain:	parameters of the medium:	description:
$\Omega^+_\delta, \Omega^+$	β_0^+, μ_0^+	const.
$\Omega^-_\delta \setminus \Omega_c$	β_0^-, μ_0^-	const.
$\Omega^- \setminus \Omega_c$	β_0^-, μ_0^-	const.
Ω_c	β, μ	pcw. const. func.
$\Omega^\varepsilon_\delta$	$\beta^{\varepsilon\delta}, \mu^{\varepsilon\delta}$	pcw. const. func.

We shall discus the following alternative definition of the cloaking problem with heterogeneous transmission layer:

1. **the δ-formulation – the layer is not homogenized**, $\Omega^G = \Omega^-_\delta \cup \Omega_\delta \cup \Omega^+_\delta$ (disjoined subdomains) and the observation manifold $\Gamma_s \subset \partial\Omega^G$ is located far away from Ω^-_δ.

2. **the homogenized formulation with the far-field cloaking effect**, i.e. the layer is represented by homogenized material distributed on $\Gamma_0 = \partial\Omega^+ \cap \partial\Omega^-$ and the manifold Γ_s is defined as above.

3. **the homogenized formulation with the strong cloaking effect**, in this case the cloaking effect is examined on the "exterior surface" of Γ^+, thus no scattered field component is observed in Ω^+.

In general there is the scattered field in Ω^+ given as $u^{\mathrm{sc}} = u - u^{\mathrm{inc}}$, i.e as the subtraction of the total and the incident field. A physically reasonable measure of the cloaking effect is the extinction function defined for a cylindric particle of unit length as:

$$Q^{\mathrm{ext}}_{\partial\Omega} = \frac{1}{d}\mathrm{Re}\left\{\int_{\partial\Omega}\left(\mathbf{n}\cdot\mathbf{d}u^{\mathrm{inc}}\overline{u^{\mathrm{sc}}} + \frac{\mathrm{j}\gamma}{k^{\mathrm{inc}}}u^{\mathrm{sc}}\overline{u^{\mathrm{inc}}}\right)\mathrm{d}l\right\} . \tag{108}$$

where k^{inc} is the incidence wavenumber, d is the effective diameter of the cross-sectional area of the particle projected onto a plane perpendicular to the direction of propagation $\mathbf{d}$ and $\gamma = \mathrm{j}\kappa + \dfrac{1}{2R}$, $\mathbf{n}$ is the outer normal unit vector, R is the radius of $\partial\Omega^G$.

The extinction function will be derived and its structure explained in the next section.

Far field cloaking observation for non-homogenized layer. The cloaking structure is situated in domain Ω_δ which is locally periodic in the sense we discussed above. The global domain, Ω^G, consists of three disjoint parts: $\Omega^G = \Omega_\delta^+ \cup \Omega_\delta \cup \Omega_\delta^-$, see Fig (15). The objects to conceal are located in Ω_δ^-, whereas on Γ_s the cloaking effect is evaluated using extinction function (108).

We assume that in Ω_δ^+ the material is homogeneous (material parameters labeled by subscript 0), whereas in $\Omega_\delta \cup \Omega_\delta^-$ the material is heterogeneous in general. However, to be consistent with the assumption considered in the next paragraph, we require that $\mu = \mu_0^\pm$, $\beta = \beta_0^\pm$ and $\sigma = \sigma_0^\pm$ on the respective interfaces $\Gamma_\delta^\pm$. The state problem has the following structure:

$$
\begin{aligned}
\frac{1}{\beta_0^+}\nabla^2 u^{\delta+} + \omega^2\mu_0 u^{\delta+} &= 0 \quad \text{in } \Omega_\delta^+ \ ,\\
\nabla\cdot\left(\frac{1}{\beta}\nabla u^{\delta-}\right) + \omega^2\mu u^{\delta-} &= 0 \quad \text{in } \Omega_\delta^- \ ,\\
\nabla\cdot\left(\frac{1}{\beta}\nabla u^{\delta}\right) + \omega^2\mu u^{\delta} &= 0 \quad \text{in } \Omega_\delta \ ,
\end{aligned}
$$

standard transmission conditions:

$$
\begin{aligned}
\partial_n(u^{\delta+} - u^\delta) &= 0 \text{ on } \Gamma_\delta^+ \ ,\\
\partial_n(u^{\delta-} - u^\delta) &= 0 \text{ on } \Gamma_\delta^- \ ,\\
u^{\delta+} - u^\delta &= 0 \text{ on } \Gamma_\delta^+ \ ,\\
u^{\delta-} - u^\delta &= 0 \text{ on } \Gamma_\delta^- \ ,
\end{aligned}
$$

boundary conditions:

$$\partial_n u^{\mathrm{sc}} - \gamma u^{\mathrm{sc}} = 0 \,\mathrm{on}\, \partial\Omega^G,$$

where

$$u^{\mathrm{sc}} = u^{\delta+} - u^{\mathrm{inc}}. \tag{109}$$

The cloaking effect can be achieved by minimization of $Q^{\mathrm{ext}}_{\Gamma_s}(u^{\mathrm{inc}}, u^{\mathrm{sc}})$.

The corresponding optimization problem can be treated as a *free material optimization problem* as follows.

$$
\begin{cases}
\quad \min\limits_{\beta,\mu} Q_{\Omega_s}(u^{\mathrm{inc}}, u^{\mathrm{sc}}) \text{ s.t.}\\
(u^{\delta+}, u^{\delta-}, u^\delta) \text{ satisfies (109)}\\
\qquad (\beta,\mu) \in \mathscr{U}_{\mathrm{ad}} \ ,
\end{cases} \tag{110}
$$

where $\mathscr{U}_{\mathrm{ad}}$ has to be specified. In particular, β,μ are fixed on the object to be cloaked (Ω_c) an can be chosen out of a set of materials in $\Omega_\delta^- \setminus \Omega_c =: \Omega_{\delta,c}^-$. The so-called free material optimization problem would amount to require

$$\mathscr{U}_{\mathrm{ad}} := \{a \in L^\infty(\Omega_{\,\mathrm{design}}; \mathbb{S}^3) | a_l \le a \le a_u, \mathrm{tr}\, a \le V\}$$

for positive semi-definite matrices $a_0, a_u \in \mathbb{S}^3$. Existence of solutions and approximation properties with respect to H-convergence have been shown in a different context by Haslinger, Kocvara, Leugering, Stingl[18]. However, the realization of H-limits is well known to be a nontrivial problem. See however [18] for a numerical approximation analysis. The application of free material optimization to the cloaking problem (110) is under way. An alternative to treat the cloaking problem for (109) is to parametrize the material properties as well as the shapes of the inclusions and possible holes in the layer $\Omega_{\delta,c}^-$ and view the problem as a nonlinear finite dimensional constrained optimization problem in reduced form, in which the the problem (109) is solved for the given data and parameter set. In particular on the level of a suitable finite-element-discretization one can derive sensitivities of the cost-function with respect to the parameters by fairly standard means. Again, the numerical treatment is under way.

Far field cloaking observation for homogenized layer. We consider the domain $\Omega^G = \Omega^+ \cup \Omega^- \cup \Gamma_0$, where $\Gamma_0 = \partial\Omega^+ \cap \partial\Omega^-$ can be curved as the straightforward generalization of the transmission layer model. Therefore, we shall introduce the the local coordinate system $(\tau,\nu)_X$ for any $X \in \Gamma_0$ where τ and ν are, respectively, the coordinates in the tangential and normal directions w.r.t. curve Γ_0 at position X. As above, the objects to conceal are located in Ω^-, see Fig. (15). On the rest of $\partial\Omega^G$, the radiation condition can be prescribed. The total field in $\Gamma_s \subset \partial\Omega^G$ is obtained by solving the following problem (we assume that in Ω^+ the medium is homogeneous, possibly air):

$$
\begin{aligned}
\frac{1}{\beta_0^+}\nabla^2 u^+ + \omega^2\mu_0 u^+ &= 0 \quad \text{in } \Omega^+ \ ,\\
\nabla\cdot\left(\frac{1}{\beta}\nabla u^-\right) + \omega^2\mu u^- &= 0 \quad \text{in } \Omega^- \ ,
\end{aligned} \tag{111}
$$

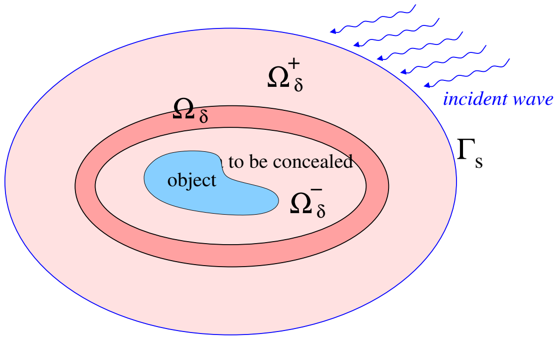

Fig. (15): Illustration to the cloaking problem formulation: for finite thickness layer Ω_δ, (109). Domain Ω^- contains the object to be cloaked by surface Γ_0 containing the metamaterial. Cloaking effect is evaluated on Γ_s.

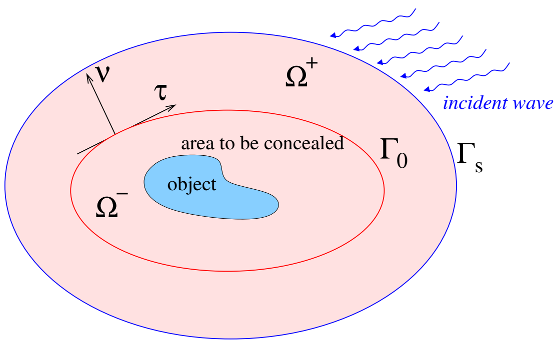

Fig. (16): Illustration to the cloaking problem formulation: for the homogenized layer represented by Γ_0, (111)

transmission conditions – Neumann type:

$$\begin{aligned} -\partial_\nu u^+ = \partial_\nu^+ u^+ = -\mathrm{j}\omega\beta_0^+ g^0 \quad & \text{on } \Gamma_0 \,, \\ \partial_\nu u^- = \partial_\nu^- u^- = \mathrm{j}\omega\beta_0^- g^0 \quad & \text{on } \Gamma_0 \,, \end{aligned} \tag{112}$$

wave transmission through the layer – jump control:

$$\begin{aligned} \partial_\tau\left(A\partial_\tau u^0 + \mathrm{j}\omega B g^0\right) + \omega^2\mu\rho^* u^0 = 0 \quad & \text{on } \Gamma_0 \,, \\ \mathrm{j}\omega B\partial_\tau u^0 + \omega^2 F g^0 = -\frac{\mathrm{j}\omega}{\delta_0}(u^+ - u^-) & \\ & \text{on } \Gamma_0 \,, \end{aligned} \tag{113}$$

boundary conditions:

$$\partial_n u^{\mathrm{sc}} - \gamma u^{\mathrm{sc}} = 0 \,\text{on}\, \partial\Omega^G . \tag{114}$$

Above in the wave transmission condition we employed (107) with $G^\pm = 0$, i.e. $\zeta_0 = 0$.
As well as in the previous case, in this situation, the cloaking effect can be achieved by minimization of $Q^{ext}_{\Gamma_s}(u^{\mathrm{inc}}, u^{\mathrm{sc}})$. In other words, one is looking for the solutions of the following problem

$$\begin{cases} \min_{\beta,\mu} Q^{\mathrm{ext}}_{\Gamma_s}(u^{\mathrm{inc}}, u^{\mathrm{sc}}) \text{ s.t.} \\ (u^{\delta+}, u^{\delta-}, u^\delta) \text{ satisfies } (111)-(114) \\ (A, B, F, \beta, \mu) \in \mathscr{U}_{\mathrm{ad}} \,, \end{cases} \tag{115}$$

where the optimization is with respect to a class of admissible functions A, B, F appearing in the transmission condition and μ, β as before. In order to understand in particular the transmission conditions along Γ_0 in (113) we focus on

$$\begin{aligned} \partial_\tau\left(A\partial_\tau u^0 + \mathrm{j}\omega B g^0\right) + \omega^2\mu\rho^* u^0 = 0 \quad & \text{on } \Gamma_0 \,, \\ \mathrm{j}\omega B\partial_\tau u^0 + \omega^2 F g^0 = -\frac{\mathrm{j}\omega}{\delta_0}(u^+ - u^-) & \\ & \text{on } \Gamma_0 . \end{aligned} \tag{116}$$

The first equation contains a Laplace-Beltrami-Helmholtz equation on Γ_0. Indeed, we define the operator

$$\begin{aligned} & T_A : L^2(\Gamma_0) \to L^2(\Gamma_0), \\ & D(T_A) := \{u \in H^1_\#(\Gamma_0) | A\partial_\tau u \in H^1(\Gamma_0)\}, \\ & T_A u := -\partial_\tau A \partial_\tau u \end{aligned} \tag{117}$$

The operator T_A is self-adjoint and positive semi-definite with discrete spectrum. The equation to solve is now

$$-T_A u + \omega^2\mu\rho^* u = -\mathrm{j}\omega\partial_\tau B g^0 .$$

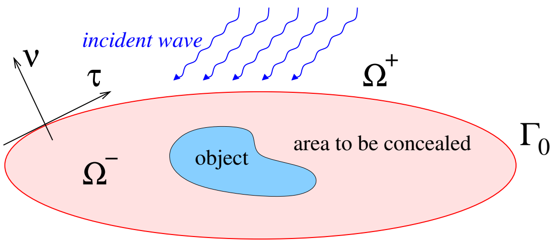

Fig. (17): Illustration to the problem formulation (121). Domain Ω^- contains the object to be cloaked by surface Γ_0 containing the metamaterial.

We introduce the resolvent $R(\lambda, T_A) := (\lambda I - T_A)^{-1}$ of T_A at a point $\lambda \in \rho(T_A)$. With this notation the first equation in (116) can be solved for u^0 as follows.

$$u^0 = -\mathrm{j}\omega R(\omega^2 \mu \rho^*, T_A)\partial_\tau B g^0, \tag{118}$$

while the second equation in (116) turns into

$$B\partial_\tau R(\omega^2\mu\rho^*)\partial_\tau B g^0 + F g^0 = \frac{1}{\mathrm{j}\omega}(u^+ - u^-), \quad \text{on } \Gamma_0. \tag{119}$$

Equation (119) is an integral equation of the second kind which admits a unique solution g^0. If one then inserts g^0 into the Neumann conditions of (112) one obtains a nonlocal transmission condition along Γ_0 which contains the functions A, B, F, μ as material parameters to be used in the optimization. The optimization problem (115) has not yet been fully explored. This will be subject to a forthcoming publication.

Strong form of the cloaking problem. We keep the domain $\Omega^G = \Omega^+ \cup \Omega^- \cup \Gamma_0$, the objects to conceal are located in Ω^-, as before. The incident wave is imposed in Ω^+. We impose the incident wave in Ω^+; let u^{inc} be the local amplitude of the plane wave, then

$$\mathrm{j}\omega\beta_0 g^0 = \partial_\nu^- u^- = \partial_\nu^+ u^+ = -k_\nu^+ u^{\text{inc}}, \tag{120}$$

where $u^\pm$ is the trace of u on $\partial\Omega^\pm \cap \Gamma_0$ and k_ν is the projection of the wave vector to the unit outward normal ν. Above $\int_{I_y^+} g^{1+} = 0$ applies due to the form of the incident wave. As the consequence, $\int_{I_y^-} g^{1-} = 0$ results by $G^\pm \equiv 0$, see (106) and (107). We consider the problem imposed in Ω^-, being defined in terms of triplet (u, u^0, g^0) which satisfies the following coupled system: wave in cloaked region:

$$\begin{aligned} \nabla\left(\frac{1}{\beta}\nabla u\right) + \omega^2\mu u = 0 \text{ in } \Omega^- \\ \partial_\nu u = \mathrm{j}\omega\beta_0^- g^0 \text{ on } \Gamma_0, \end{aligned} \tag{121}$$

wave transmission through the layer:

$$\begin{aligned} \partial_\tau\left(A\partial_\tau u^0 + \mathrm{j}\omega B g^0\right) + \omega^2\mu\rho^* u^0 = 0 \quad \text{on } \Gamma_0, \\ \mathrm{j}\omega B\partial_\tau u^0 + \omega^2 F g^0 = -\frac{\mathrm{j}\omega}{\delta_0}(u^{\text{inc}} - u) \\ \text{on } \Gamma_0. \end{aligned} \tag{122}$$

In fact the *cloaking condition* (120) can be viewed as an exact controllability constraint with variables (A, B, F), the coefficients of the homogenized transmission through the heterogeneous layer, as controls. This exact controllability problem can be solved for special scenarios. However, in general we cannot expect exact controllability, and therefore the controllability constraint has to be relaxed by an appropriate optimization with penalty.
In general, the flux g^0 obtained by solving (121), (122) i.e. as the *State Problem* solution, is not consistent with the incident wave assumed in Ω^+; it fits the assumption of "no reflection", when

$$0 = k_\nu^+ u^{\text{inc}} + \mathrm{j}\omega\beta_0 g^0, \quad \text{a.e. on } \Gamma_0,$$

therefore, the *cloaking effect* can be approached by the following minimization:

$$\min_{A,B,F} \Psi(g^0, A, B, F), \tag{123}$$

where $\Psi = \|k_\nu^+ u^{\text{inc}} + \mathrm{j}\omega\beta_0 g^0\|_{\Gamma_0}$, s.t. g^0 solves the *State Problem* (121) with (122) for given u^{inc}.
Coefficients (A, B, F) can be handled by designing the microstructure in cell Y.

Remark 4. In general, there is the jump on Γ_0, $[u]_{\Gamma_0} = u^+ - u^- \not\equiv 0$. u^0 involved in (122) is an internal variable which is relevant only if $B \not\equiv 0$ on Γ_0; otherwise (122) reduces to

$$\omega^2 F g^0 + \frac{\mathrm{j}\omega}{\delta_0}(u^{\text{inc}} - u) = 0 \quad \text{on } \Gamma_0.$$

In this case the problem (121), (122) reduces to a Helmholtz-problem

$$\begin{cases} \nabla\frac{1}{\beta}\nabla u + \omega^2\mu u = 0 \ \text{ in } \Omega^- \\ \partial_\nu u + \alpha u = \alpha u^{\text{inc}} \ \text{ on } \Gamma_0 \end{cases}$$

with local Robin-type boundary condition on Γ_0. The cloaking constraint then also reduces to just another boundary condition on Γ_0. This leads to an overdetermined boundary value problem which may or not may have a solution.

$\triangle$

TOPOLOGY OPTIMIZATION FOR THE CLOAKING PROBLEM

In this section we would like to demonstrate the topology optimization method to design a cloaking layer such that the given object will become less visible.

Let us consider a small object (i.e. a nanoparticle composed from a given material). Our aim is to design a topology of a cloaking layer (composite of the matrix medium and a medium with a low refractive index) in such a way that for an observer (sensor) present behind the particle, the particle becomes in some sense (specified by a cost function) invisible. Propagation of the electromagnetic waves in the composite is described by the Helmholtz equation (as defined in the previous sections). The geometry of the problem is described by figure (18). The state equation is considered in a circular domain $\overline{\Omega} = \cup_{i=1}^{3} \overline{\Omega}_i$ with the boundary $\partial\Omega$. We place a particle (characterized by a complex refractive index) in the middle of the computational domain. Its body is included in the set $\overline{\Omega}_1$. The particle is coated by a shell (Ω_2). And the core-shell is in turn embedded into a matrix medium (Ω_3).

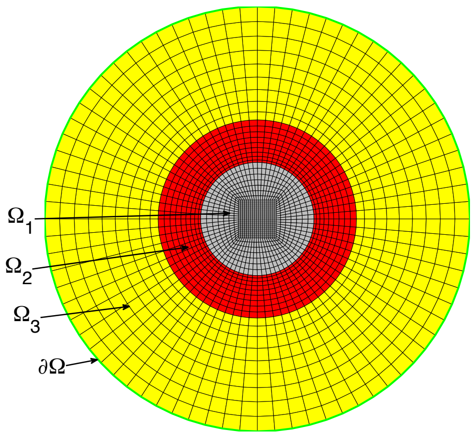

Fig. (18): Description of geometry for the strong form of cloaking problem

The refractive index is supposed to be constant in subdomains Ω_1, Ω_3, but is changing across interfaces and may vary in Ω_2. Since we will solve the Helmholtz equation on a finite computational domain we have to define appropriate boundary conditions. These conditions should prevent occurrence of non-physical reflections from the artificial boundary (i. e. the outer boundary should be transparent for the scattered field or the boundary conditions should absorb the scattered wave, that's why in the following we will call them absorbing boundary conditions). There are various ways in which such conditions can be chosen, we have used a.b.c. of first order for it's simplicity, these conditions retains sparsity of the finite element system matrix, on the other hand, they do not prevent reflections for all directions of incidence. The total rescaled electric Hertz potential u may be decomposed into the incident and the scattered field

$$u = u^{\mathrm{inc}} + u^{\mathrm{sc}}, u^{\mathrm{inc}} = e^{-\mathrm{j}\kappa^{\mathrm{inc}}\mathbf{d}\cdot\mathbf{x}}, \tag{124}$$

where $\mathbf{d}$ is the direction of propagation of the incident wave. Furthermore we observe

$$\nabla u^{\mathrm{inc}} = -\mathrm{j}\kappa^{\mathrm{inc}}\mathbf{d}u^{\mathrm{inc}}. \tag{125}$$

The absorbing b.c. give the relation between the scattered field and its derivative in the direction of the outer normal on the boundary

$$\partial_n u^{\mathrm{sc}} - \gamma u^{\mathrm{sc}} = 0 \,\mathrm{on}\, \partial\Omega, \tag{126}$$

where $\gamma = \mathrm{j}\kappa + \dfrac{1}{2R}$. The Helmholtz equation has than the following form

$$\left\{ \begin{array}{rl} \nabla \cdot \left(\dfrac{1}{\beta_r} \nabla u \right) + \kappa_0^2 \mu_r u & = 0 \,\mathrm{in}\, \Omega, \\ \left[\dfrac{1}{\beta_r} \partial_n u \right]_\Gamma & = 0 \,\mathrm{on}\, \Gamma, \\ [u]_\Gamma & = 0 \,\mathrm{on}\, \Gamma, \\ \partial_n u^{\mathrm{sc}} - \gamma u^{\mathrm{sc}} & = 0 \,\mathrm{on}\, \partial\Omega, \end{array} \right. \tag{127}$$

where $\beta_r = n^2$ is the complex relative permittivity (square of the refractive index).

Remark 5. The total (or also scattered) potential $u(u^{\mathrm{sc}})$ depends generally on the frequency $\omega \in \Lambda$ and on the direction of propagation $\mathbf{d} = (\cos\alpha, \sin\alpha), \alpha \in \Sigma$, where $\Lambda = \{\omega_1, \ldots, \omega_n\}$ is a set of given frequencies, $\Sigma = \{\alpha_1, \ldots, \alpha_m\}$ is the set of angles of incidence.

$\triangle$

To obtain the weak form of Helmholtz equation we multiply $(127)_1$ by the test function $v \in H(\Omega)$, where $H(\Omega)$ is the standard Sobolev space

$$H(\Omega) = W^{1,2} = \left\{ v | v, \frac{\partial v}{\partial x_i} \in L^2(\Omega), i = 1,2 \right\}. \tag{128}$$

We apply the Green's theorem, further we use (124), $(127)_4$ and (125). Then the weak formulation may be written as follows

$$\left\{ \begin{array}{l} \text{Find } u^{\mathrm{sc}} \in H(\Omega) \text{ such that for all } v \in H(\Omega) \text{ holds} \\ a(u^{\mathrm{sc}}, v) = f(v). \end{array} \right. \tag{129}$$

where a sesquilinear form $a : H \times H \to \mathbf{C}$ is defined as

$$a(u^{\mathrm{sc}}, v) = -\int_\Omega \frac{1}{\beta_r} \nabla u^{\mathrm{sc}} \overline{\nabla v} \,\mathrm{d}S + \int_\Omega \kappa_0^2 \mu_r u^{\mathrm{sc}} \overline{v} \,\mathrm{d}S + \int_{\partial\Omega} \frac{1}{\beta_r} \gamma u^{\mathrm{sc}} \overline{v} \,\mathrm{d}l \tag{130}$$

and the operator $f(\cdot)$ is the operator of the right hand side $f : H \to \mathbf{C}$

$$f(v) = \int_\Omega \frac{1}{\beta_r} \nabla u^{\mathrm{inc}} \overline{\nabla v} \,\mathrm{d}S - \int_\Omega \kappa_0^2 \mu_r u^{\mathrm{inc}} \overline{v} \,\mathrm{d}S + \int_{\partial\Omega} \frac{1}{\beta_r} \mathbf{n} \cdot \mathbf{d} \mathrm{j} \kappa^{\mathrm{inc}} u^{\mathrm{inc}} \overline{v} \,\mathrm{d}l \quad \forall v \in H(\Omega). \tag{131}$$

Cost functional

Our aim is to minimize the so-called extinction efficiency. That is a function that reflects energy loss due to the inserted particle.

Energy flux at any point of space is represented by the Poynting vector

$$\mathbf{S} = \frac{1}{2} \mathrm{Re} \left\{ \boldsymbol{E} \times \overline{\boldsymbol{H}} \right\}. \tag{132}$$

In the following we will define the energy that is scattered, absorbed and extincted per unit length of the cylinder L. We will ignore effects of the ends of the cylinder. Now imagine a fictive cylinder around the particle (in our concept it will be represented by the boundary of the computational domain $\partial\Omega$). We define net rate W^{abs} at which the electromagnetic energy crosses $\partial\Omega$

$$W^{\mathrm{abs}} = -L \int_{\partial\Omega} \mathbf{S} \cdot \mathbf{n} \,\mathrm{d}l. \tag{133}$$

If $W^{\mathrm{abs}} > 0$ energy is absorbed in Ω, if $W^{\mathrm{abs}} < 0$ energy is created in Ω (not considered in the following).

The absorbed energy rate W^{abs} may be decomposed into the incident energy rate (identically zero), extincted and scattered energy rates

$$W^{\mathrm{abs}} = W^{\mathrm{inc}} + W^{\mathrm{ext}} - W^{\mathrm{sc}} \tag{134}$$

Extinction efficiency is then defined as

$$Q^{\mathrm{ext}} = \frac{1}{G I^{\mathrm{inc}}} W^{\mathrm{ext}}, \tag{135}$$

where I^{inc} is incident irradiance - magnitude of the Poynting vector of the incident wave

$$I^{\mathrm{inc}} = |\mathbf{S}^{\mathrm{inc}}| = \frac{1}{2} \left| \mathrm{Re} \left\{ \boldsymbol{E}^{\mathrm{inc}} \times \overline{\boldsymbol{H}}^{\mathrm{inc}} \right\} \right| \tag{136}$$

and $G = Ld$ is cross-sectional area of the particle projected onto a plane perpendicular to the direction of propagation (d is the diameter of the shelled particle).

In the following we will formulate the extinction efficiency in terms of the state variable u^{sc}. The magnetic end electric field intensities for a homogeneous and non-absorbing medium ($\beta = const > 0$) may be rewritten as follows

$$\boldsymbol{E} = \frac{1}{\omega^2 \beta} \nabla \times (u \mathbf{e}_3) = -\frac{1}{\omega^2 \beta} \mathbf{e}_3 \times \nabla u, \tag{137}$$

$$\boldsymbol{H} = (\sigma - \mathrm{j} \varepsilon \omega) \frac{1}{\omega^2 \beta} u \mathbf{e}_3 = -\frac{\mathrm{j}}{\omega} u \mathbf{e}_3. \tag{138}$$

Then the Poynting vector may be rewritten as follows (noting that $\mathbf{e}_3 \cdot \nabla u = 0$)

$$\begin{aligned} \mathbf{S} &= -\frac{1}{2\omega^3 \beta} \mathrm{Re} \left\{ \mathrm{j} \left(\mathbf{e}_3 \times \nabla u \right) \times \overline{u} \mathbf{e}_3 \right\}, \\ &= -\frac{1}{2\omega^3 \beta} \mathrm{Re} \left\{ \mathrm{j} \overline{u} \nabla u \right\}. \end{aligned} \tag{139}$$

The incident irradiance is then given by (using (125))

$$I^{\mathrm{inc}} = \frac{1}{2} \left| \mathrm{Re} \left\{ \boldsymbol{E}^{\mathrm{inc}} \times \overline{\boldsymbol{H}^{\mathrm{inc}}} \right\} \right| = \frac{k^{\mathrm{inc}}}{2\omega^3 \beta}. \tag{140}$$

Using (139) also extinction energy rate is obtained as (using $(127)_4$ and again (125))

$$\begin{aligned} W^{\mathrm{ext}} &= \frac{L}{2\omega^3 \beta} \int_{\partial\Omega} \mathrm{Re} \left\{ \mathrm{j} \overline{u^{\mathrm{sc}}} \nabla u^{\mathrm{inc}} + \mathrm{j} \overline{u^{\mathrm{inc}}} \nabla u^{\mathrm{sc}} \right\} \cdot \mathbf{n} \,\mathrm{d}l, \\ &= \frac{L}{2\omega^3 \beta} \int_{\partial\Omega} \mathrm{Re} \left\{ \mathbf{n} \cdot \mathbf{d} k^{\mathrm{inc}} u^{\mathrm{inc}} \overline{u^{\mathrm{sc}}} + \mathrm{j} \gamma u^{\mathrm{sc}} \overline{u^{\mathrm{inc}}} \right\} \mathrm{d}l. \end{aligned} \tag{141}$$

Using (135) the final formula for the extinction efficiency is obtained as

$$Q^{\mathrm{ext}} = \frac{1}{d} \mathrm{Re} \left\{ \int_{\partial\Omega} \left(\mathbf{n} \cdot \mathbf{d} u^{\mathrm{inc}} \overline{u^{\mathrm{sc}}} + \frac{\mathrm{j}\gamma}{k^{\mathrm{inc}}} u^{\mathrm{sc}} \overline{u^{\mathrm{inc}}} \right) \mathrm{d}l \right\}. \tag{142}$$

Min-max problem

The aim of the optimization is to minimize values of the cost functional for a selected interval of frequencies. It can be achieved by the worst scenario approach: we shall minimize the cost functional value for the worst case frequency.
We would like to find an optimal distribution of two isotropic materials characterized with refractive indices n_0, n_1. This leads to the discrete optimization, which is generally a very difficult problem. One possibility to handle this problem is to introduce relaxation of the material (the SIMP method, [5]). We define pseudo density function $\rho(\mathbf{x}) \in \mathscr{U}_{ad}$

$$\begin{aligned} n(\rho(\mathbf{x}),\omega) &= n_0(\omega) + (n_1(\omega) - n_0(\omega))\rho(\mathbf{x})^p, \\ & p > 1, \\ \mathscr{U}_{ad} &= \left\{ \frac{1}{|\Omega_2|} \int_{\Omega_2} \rho(\mathbf{x})\,\mathrm{d}S \le \rho^*, \right. \\ & \left. 0 \le \rho(\mathbf{x}) \le 1, \mathbf{x} \in \Omega_2 \right\}, \end{aligned} \tag{143}$$

where $\mathscr{U}_{ad}$ is the admissible set, ρ^* is the maximal fraction of the material with refractive index n_1 that may be included in the design layer. The worst scenario approach may be formulated as follows

$$\min_{\rho \in \mathscr{U}_{ad}} \max_{\omega \in [\omega_1, \omega_n], \alpha \in [\alpha_1, \alpha_m]} \Psi(u^{\mathrm{sc}}_{\omega,\alpha}), \tag{144}$$

where Ψ is the cost functional depending on the state variable.
For the finite element analysis we have to define the discrete form of the previous problem. Let E be a set of indices of finite elements in the design subdomain Ω_2. Then the refractive index for every finite element in E is defined as follows

$$\begin{aligned} n_e(\omega) &= n_0(\omega) + (n_1(\omega) - n_0(\omega))\rho_e^p,\ p > 1, \\ \hat{\rho}(\mathbf{x}) &= \sum_{e \in E} \rho_e \chi_e(\mathbf{x}), \hat{\rho} \in \widetilde{\mathscr{U}_{ad}} \\ \widetilde{\mathscr{U}_{ad}} &= \left\{ card(E) \sum_{e \in E} \rho_e \le \rho^*, \right. \\ & \left. 0 \le \rho_e \le 1\, \forall e \in E \right\}, \end{aligned} \tag{145}$$

where χ_e is a characteristic function of the finite element e in Ω_2, $card(E)$ is the amount of finite elements in the design layer. The problem (144) is then in then reformulated as follows

$$\min_{\hat{\rho} \in \widetilde{\mathscr{U}_{ad}}} \max_{\omega \in \Lambda, \alpha \in \Sigma} \Psi(u^{\mathrm{sc}}_{\omega,\alpha}). \tag{146}$$

The Method of Moving Asymptotes (MMA) is used to solve the preceding problem. One additional reformulation of (146) is necessary

$$\min_{\hat{\rho} \in \widetilde{\mathscr{U}_{ad}}} c \tag{147}$$

subject to:

$$\begin{aligned} h_{i,j} &\le 0, \quad i = 1,\dots,n, j = 1,\dots,m, \\ g &\le 0, \\ 0 \le \rho_e &\le 1, \quad \forall e \in E, \end{aligned} \tag{148}$$

where

$$\begin{aligned} h_{i,j} &= \Psi(u^{\mathrm{sc}}_{\omega_i,\alpha_j}), \omega_i \in \Lambda, \alpha_j \in \Sigma \\ & \text{for } i = 1,\dots,n, j = 1,\dots,m, \\ g &= \frac{1}{card(E)} \textstyle\sum_{e \in E} \rho_e - \rho^*. \end{aligned} \tag{149}$$

The MMA method requires knowledge of the gradient of the cost functional which is obtained via the sensitivity analysis. Sensitivity analysis of similar problems is provided in a detailed way in [40] or [32].
The main task is the solution of the adjoint equations (that are in fact optimality conditions of the Lagrangian $\mathscr{L}$ of our problem), the equations are formally defined as follows

$$\left\{ \begin{array}{l} \text{Find } w \in H(\Omega) \text{ such that for all } v \in H(\Omega) \text{ holds} \\ (\delta_{Re}\psi(u^{\mathrm{sc}}) - j\delta_{Im}\psi(u^{\mathrm{sc}})) \cdot v + a(v,w) = 0. \end{array} \right. \tag{150}$$

Then the final sensitivity of the cost functional for a given frequency ω and an angle of incidence α is formulated as

$$\begin{aligned} \delta\psi = \delta\mathscr{L}(\rho, u^{\mathrm{sc}}, w) &= \delta_\rho\left(a(u^{\mathrm{sc}}, w) - f(w)\right) \\ &= \delta_\rho\left(a(u,w)\right), \\ &= \int_{\Omega_D} -2n_e(\rho_e)^{-3} p(n_1 - n_0)\rho_e^{p-1} \nabla u \overline{\nabla w}\,\mathrm{d}S. \end{aligned} \tag{151}$$

Implementation and results

The discretization of the state equations was done by the classical approach of the finite element method (for details we recommend the well known book Zienkiewicz et.al. [47]). The state equation is solved by the finite element method using isoparametric, bilinear, hexahedral finite elements (an introduction is given by Jianming Jin in [19]).

In all following examples the extinction efficiency was minimized ($\Psi = Q^{\text{ext}}$), although the scattering efficiency would be also a good alternative, since

$$Q^{\text{ext}} = Q^{\text{abs}} + Q^{\text{sc}} \tag{152}$$

and we observed the decrease of the extinction was mainly due to lower scattering than absorption.
On figure (19) we may observe a particle with higher refractive index (2.1) that is surrounded by the layer with refractive index given by the pseudo density $\rho = 0.3$. Dark blue color in the shell corresponds to the matrix material ($n = 1.31$), by the red color low refractive index material is represented ($n = 0.95$, that is more or less air). We see that the design evolves to two oval inclusions ((24)), which maintains more than 60 % decrease in extinction.

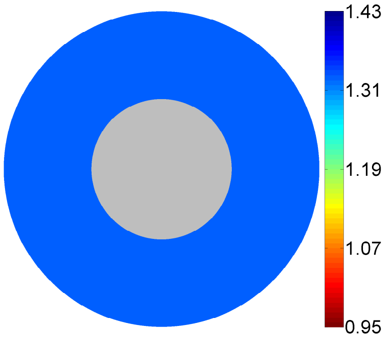

Fig. (19): Initial design - iteration 0.

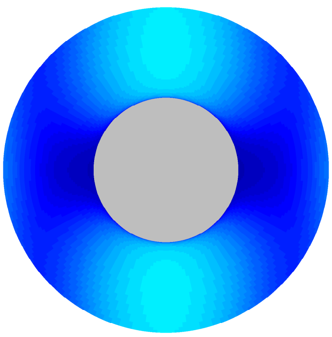

Fig. (20): Design - iteration 6.

The extinction efficiency curves for particular iterations are displayed on figure (25). The pink interrupted curve corresponds to the bare particle.
The inclusions in the final design (24) have no clear interface with respect to the matrix medium. The production of such shell is out of reach of nowadays technology. Our suggestion is to use the optimal topology design as an initial guess for the shape

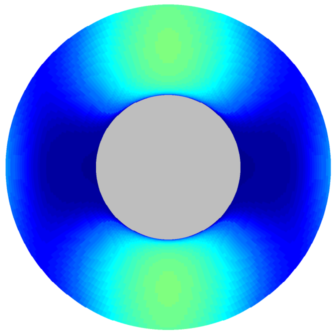

Fig. (21): Design - iteration 9.

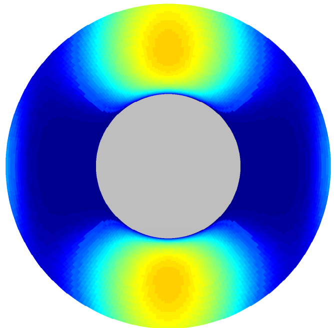

Fig. (22): Design - iteration 12.

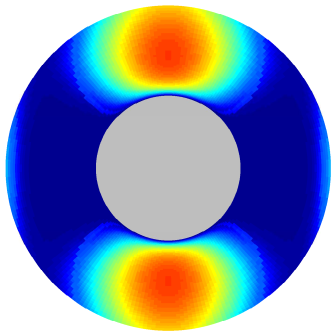

Fig. (23): Design - iteration 14.

optimization method. On Figures. (26), (27) the contour lines and initial shape of 3 layers with piecewise constant refractive index are defined. The geometry of such structure could be parametrized and optimized in a similar way as was published in [39], [40].
Finally the optimal design for two, three and four angles of incidence is displayed on figures (28), (29) and (30). Of course the decrease of extinction is not so huge as in the previous simulation, but we still get improvement approximately 20-40 %. The complicated structures that develop give us hint back to

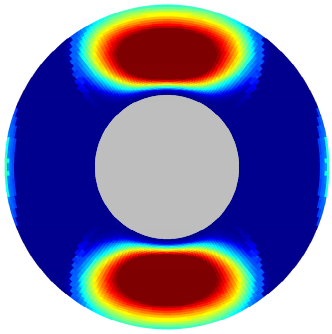

Fig. (24): Design - iteration 18.

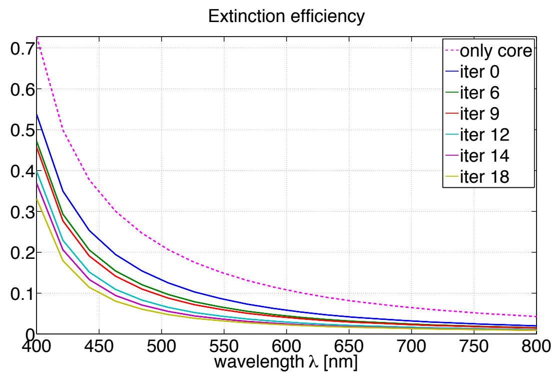

Fig. (25): Cost functional values for particular iterations

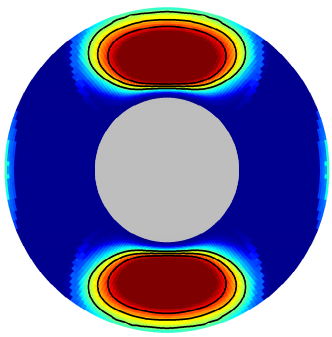

Fig. (26): Contour lines..

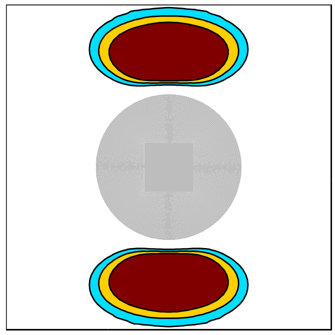

Fig. (27): Contour layers.

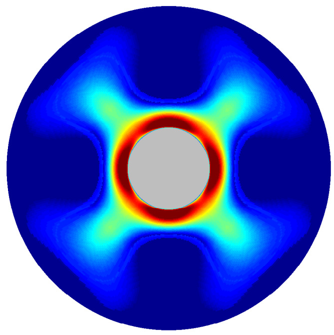

Fig. (28): Optimal design for 2 directions, $\Sigma = \{-1/4\pi, 1/4\pi\}$.

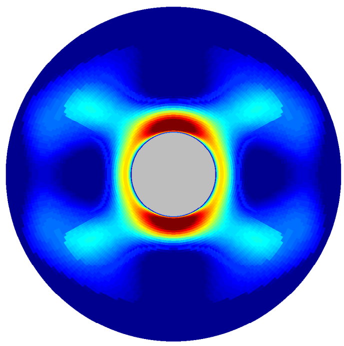

Fig. (29): Optimal design for 3 directions, $\Sigma = \{-1/4\pi, 0, 1/4\pi\}$.

the previous section (Fig. (15)). We believe that the optimally designed micro-structure would reduce the extinction even more significantly than has been shown on Fig. (25).

CONCLUSION

As we have amply demonstrated, meta-materials in the acoustic, electromagnetic, elastic and piezoelectric context can be approached by quite analogous mathematical methods. Therefore, a unifying theory of meta-materials for wave propagation is within reach. It turns out that micro- or nano-structured layers play an important role in obtaining meta-properties, like cloaking and band-gap phenomena. Similarly, micro-structures appear in auxetic elastic materials, like metallic or ceramic foams. In order to achieve results that lead to a an actual mechanical, acoustic or electromagnetical device, further research has to be conducted. In particular, post-processing and interpretation tools have to be

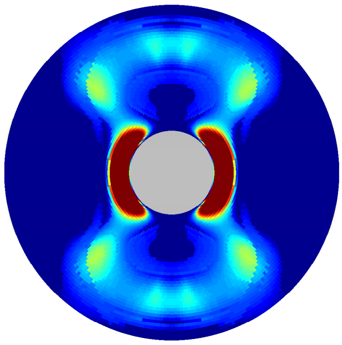

Fig. (30): Optimal design for 4 directions, $\Sigma = \{-1/2\pi, -1/3\pi, 1/3\pi, 1/2\pi\}$.

developed in order to transfer the numerical results into practice.

ACKNOWLEDGEMENT

The notion 'Engineering of Advanced Materials' implicitly announcing a program all by itself, is also the title of a research cluster within the German Excellence Initiative funded by the Deutsche Forschungsgemeinschaft (DFG). The current contribution was initiated in the Center of 'Multi-scale Modeling and Simulation' run by the first author. Second author has been visiting the institute a number of times, while the third author is employed there. The second author has been also supported by projects of the Czech Science Foundation 101/07/1417 and by project MSM 4977751301 of the Czech Ministry of Education.

REFERENCES

[1] G. Allaire, Homogenization and two-scale convergence. SIAM J Math Anal 1992; 23: 1482-1518.

[2] T. S. Angell and A. Kirsch. Optimization Methods in Electromagnetic Radiation, Springer-Verlag New York, 2004.

[3] J.L. Auriault and G. Bonnet, Dynamique des composites elastiques periodiques, Arch Mech 1985; 37: 269-284.

[4] A. Ávila, G. Griso, B. Miara and E. Rohan, Multi-scale modelling of elastic waves – theoretical justification and numerical simulation of band gaps, SIAM Multi Model Simul 2008; 7: 1-21.

[5] M. B. Bendsoe and O. Sigmund, Topology optimization, Theory, Methods and Applications, Springer-Verlag, Berlin, Heidelberg, 2003 and 2004.

[6] C.R. Bohren and D.R. Huffman, Absorption and Scattering of Light by Small Particles, Wiley-VCH, Weinheim, 2004.

[7] A. S. Bonnet-Bendhia, D. Drissi and N. Gmati, Simulation of muffler's transmission losses by a homogenized finite element method, J Comput Acous 2004; 12: 447-474.

[8] A. S. Bonnet-Bendhia, D. Drissi and N. Gmati, Mathematical analysis of the acoustic diffraction by a muffler containing perforated ducts, Math Model Meth Appl Sci 2005; 15: 1059-1090.

[9] G. Bouchitte and D. Felbacq, Homogenization near resonances and artificial magnetism from dielectrics, C.R.Acad.Sci, Ser. 2004; 1339: 377-382.

[10] R. Cimrman and E. Rohan, Three phase phononic materials, Appl. Comput Mech 2009; 3: 5-16.

[11] R. Cimrman and E. Rohan, Three-phase phononic materials. accepted : Appl. Comp. Mech., Univ. West Bohemia, Pilsen, (2009).

[12] D. Cioranescu, A. Damlamian, G. Griso and D. Onofrei, The periodic unfolding method for perforated domains and neumann sieve models, J Math Pure Appl. 2008; 89: 248-277.

[13] D. Cioranescu, A. Damlamian and G. Griso, The periodic unfolding method in homogenization, SIAM J Math Anal 2008; 40: 1585-1620.

[14] D. Cioranescu and P. Donato, An introduction to homogenization. No. 17 in Oxford Lecture Series in Mathematics and its Applications. Oxford University Press, Oxford, 1999.

[15] D. Cioranescu and J. Saint Jean Paulin, Homogenization of Reticulated Structures, Springer, Appl. Math. Ser. 136, New York, 1999.

[16] A. Greenleaf, Y. Kurylev, M. Lassas and G. Uhlmann, Approximate quantum and acoustic cloaking, arXiv:0812.1706v1[math-ph] 9 Dec 2008.

[17] M.E. Gurtin, Configurational forces as basic concept in continuum physics, Springer-Verlag, Applied Mathematical Sciences 137, 2000.

[18] J. Haslinger, M. Kocvara, G. Leugering and M. Stingl, Multidisciplinary free material optimization, submitted 2009.

[19] J. Jin, The finite element method in electromagnetics, John Wiley & Sons, Inc., New York, 2002.

[20] P. Kogut and G. Leugering, S-homogenization of optimal controls problems in Banach spaces, Math Nachr 2002; 233-234: 141-169.

[21] P. Kogut and G. Leugering, Homogenization of optimal control problems in variable domains. Principle of the fictitious homogenization, Asympt Anal 2001; 26: 37-72.

[22] P.I. Kogut and G. Leugering, Homogenization of constrained optimal control problems for one-dimensional elliptic equations on periodic graphs, ESAIM, Control Optim Calc Var 2009;15: 471-498.

[23] P.I. Kogut and G. Leugering, Homogenization of Dirichlet optimal control problems with exact partial controllability constraints, Asympt Anal 2008; 57: 229-249.

[24] V. Lukeš and E. Rohan, Computational analysis of acoustic transmission through periodically perforated interfaces, Appl Comput Mech 2009; 3: 111-120.

[25] B. Miara, E. Rohan, M. Zidi and B. Labat, Piezomaterials for bone regeneration design - homogenization approach, J Mech Phys Solids 2005; 53, 2529-2556.

[26] G. W. Milton and J. R. Willis, On modifications of Newton's second law and linear continuum elastodynamics, Proc Royal Soc. A 2007; 483: 855-880.

[27] J.B. Pendry, D. Schurig and D.R. Smith, Calculation of of material properties and ray tracing in transformation optics, Opt Eng 2006; 14: 9794.

[28] J.B. Pendry, Negative refraction makes perfect lens, Phys. Rev. Letters 2000; 85: 3966-3969.

[29] E. Rohan and V. Lukeš, Sensitivity analysis for the optimal perforation problem in acoustic transmission, Appl Comput Mech 2009; 3: 163-176.

[30] E. Rohan and R. Cimrman, Dispersion properties in homogenized piezoelectric phononic materials, In: Proceedings of the conference Engineering Mechanics 2009, Svratka 2009.

[31] E. Rohan and B. Miara, Modelling and sensitivity analysis for design of phononic crystals, PAMM, Proc Appl Math Mech 2006; 6: 505-506.

[32] E. Rohan and B. Miara, Sensitivity analysis of acoustic wave propagation in strongly heterogeneous piezoelectric composite, In: Topics on Mathematics for Smart Systems, World Scientific Publishers, 2006: 139-207.

[33] E. Rohan and B. Miara, Shape sensitivity analysis for material optimization of homogenized piezo-phononic materials, In: Proceedings of the WCSMO-8, Lisbon, Portugal 2009.

[34] E. Rohan and B. Miara, Homogenization and shape sensitivity of microstructures for design of piezoelectric bio-materials, Mech Adv Materials Struct 2006; 13: 473-485.

[35] E. Rohan, B. Miara and F. Seifrt, Numerical simulation of acoustic band gaps in homogenized elastic composites, Int J Engin Sci 2009; 47: 573-594.

[36] E. Rohan et.al., On nonsmooth sensitivity of phononic band gaps in elastic structures, in preparation.

[37] E. Rohan and G. Leugering, Homogenization of particle-cloaking layer in EM radiation, in preparation.

[38] E. Rohan and V. Lukeš, Homogenization of the acoustic transmission through perforated layer, J Appl Math Phys, (to appear 2009).

[39] F. Seifrt, G. Leugering and E. Rohan, Shape optimization for the Helmholtz equation, PAMM, Proc Appl Math Mech 2008; 8: 10705-10706.

[40] F. Seifrt, G. Leugering and E. Rohan, Tracking optimization for propagation of electromagnetic waves for multiple wavelengths, Appl Comp Mech 2008; 2: 369-378, Univ. of West Bohemia, Pilsen.
[41] E. Sanchez-Palencia, Non-homogeneous media and vibration theory, Lecture Notes in Physics 127, Springer, Berlin, 1980.
[42] A.P. Seyranian, E. Lund and N. Olhoff, Multiple eigenvalues in structural optimization problems, Struct Opt 1994; 8: 207-227.
[43] O. Sigmund and J. S. Jensen, Systematic design of phononic band-gap materials and structures by topology optimization, Phil Trans Royal Soc London, A 2003; 361: 1001-1019.
[44] V. Shalaev, Optical negative-index metamaterials, Nature Photonics 2007; 1, www.nature.com/naturephotonics
[45] D.R. Smith and J.B. Pendry, Homogenization of metamaterials by field averaging, J Opt Soc Am 2006; 23: 391-403.
[46] E. Wadbro and M. Berggren, Topology optimization of an acoustic horn, Comput Meth Appl Mech Engrg 2006; 196: 420-436.
[47] O.C. Zienkiewicz, R.L. Taylor and J.Z. Zhu, The Finite Elements Method: Its Basis and Fundamentals, Elsevier, Burlington, 2005.